Deliverable A2.1 "Indicators for the evaluation of restoration actions to combat degradation/desertification"

Project ref. number	LIFE20 PRE/IT/000007
Project title	Remote sensing oriented nature based solutions towards a NEW LIFE FOR DRYLANDS
Project Acronym	NewLife4Drylands

Deliverable title	Indicators for the evaluation of restoration actions to combat degradation/desertification
Deliverable number	2.1
Deliverable version	V1.1
Contractual date of delivery	30/09/2021
Actual date of delivery	30/09/2021
Online access	yes
Diffusion	Public
Nature of deliverable	technical
Action	A2
Partner responsible	CNR-IIA
Author(s)	Cristina Tarantino, Saverio Vicario, Maria Adamo (CNR-IIA)

	Vicenç Carabassa, Pau Montero, Joan Masó, Cristina Domingo (CREAF)
	Vito Cambria, Marcello Vitale (SAPIENZA)
	Kostis Damianakis, Kalliopi Baxevani, Michalis Probonas (UoC)
Editor	Cristina Tarantino

Executive summary

In the framework of NewLife4Drylands project, action A.2, the present document emphasises the useful contribution of remote sensing, mainly satellite-based, to provide a protocol for the assessment of land degradation at local scale. The protocol will be, also, useful to evaluate the effectiveness of sustainable solutions and restoration actions, based on Nature-Based Solutions (NBS), to combat degradation for those sites where NBS will be applied (short term monitoring) or are currently implemented by other LIFE projects (mid/long-term monitoring).

The importance to define a spatial and a temporal framework for investigation leading to the working scale and open satellite sources identification is highlighted. A set of selected well-known indicators from remote sensing is provided both with the scientific and technical procedure for their extraction from open satellite data, at a local scale, for each study site. The selection of indicators has been carried out based on scientific and technical literature, consortium members' expertise and discussions with the Advisory Board.

Table of Contents

Acronyms and Abbreviations

Acronym	Description
AOI	Area Of Interest
ARVI	Atmospherically Resistant Vegetation Index
ASI	Italian Space Agency
BI	Bare Index
CCA	Cross Correlation Analysis
CLC	Corine Land Cover
CNN	Convolutional Neural Network
DSI	Desertification Soil Index
DVI	Difference Vegetation Index
EO	Earth Observation
ECV	Essential Climate Variables
ESA(I)	Environmentally Sensitive Areas to Desertification (Index)
EU	European Union
EV	Essential Variable
EVI	Enhanced Vegetation Index
FAO-LCCS	Food and Agriculture Organisation -Land Cover Classification System
FAPAR	Fraction of Absorbed Photosynthetically Active Radiation
GCOS	Global Climate Observing System
GNDVI	Green Normalized Difference Vegetation Index
GPP	Gross Primary Production
HR	High Resolution
HR-VPP	High-Resolution Vegetation Phenology and Productivity
KBA	Key Biodiversity Areas
LAI	Leaf Area Index
LC	Land Cover
LCLU	Land Cover and Land Use
LD	Land Degradation

LDN	Land Degradation Neutrality
MNDWI	Modified Normalized Difference Water Index
MSAVI	Modified Soil Adjusted Vegetation Index
N2K	Natura 2000
NBR	Normalized Burn Ratio
NBS	Nature-Based Solutions
NDDI	Normalized Difference Drought Index
NDMI	Normalized Difference Moisture Index
NDRE	Normalized Difference RedEdge
NDBSI	Normalized Difference Bare Soil Index
NDSI	Normalized Difference Soil Index
NDVI	Normalized Difference Vegetation Index
NDWI	Normalized Difference Water Index
NIR	Near Infra-Red
NN	Neural Network
NPP	Net Primary Production
OSAVI	Optimized Soil-Adjusted Vegetation Index
PA	Protected Area
PCC	Post Classification Comparison
PP	Primary Production
PPI	Plant Phenology Index
PRI	Photochemical Reflectance Index
REP	RedEdge Position
RF	Random Forest
RS	Remote Sensing
SAR	Synthetic Aperture Radar
SASI	Soil Adjusted Salinity Index
SDG	Sustainable Development Goal
SDVI	Standardized Drought Vulnerability Index

SOC	Soil Organic Carbon
SOCI	Soil Organic Carbon Index
SI	Salinity Index
SSI	Soil Salinity Index
SVM	Support Vector Machine
SWIR	Short Wave Infra-Red
UN	United Nations
UNCCD	United Nations Convention to Combat Desertification
VHR	Very High Resolution
Vis	Visible

1.   Introduction

NewLife4Drylands project has its focus on:

- providing a framework and a protocol for identifying and monitoring Land Degradation (LD) at local scale;
- providing a specific protocol for the mid and long-term monitoring with regard to the application, scalability, replication, failures and successes of NBS for restoration interventions on degraded land.

Both protocols, developed for the 6 study sites of the project, have in common the use of Remote Sensing (RS) data and techniques.

RS can complement the lack of long term, reliable and homogeneous in situ information, usually rather time-consuming and cost expensive.

The recent availability of open satellite data (e.g., Copernicus program services), free of charge, orbiting around the Earth, acquiring at High spatial Resolution (HR), represents a relevant opportunity to obtain measurements on a large temporal and spatial scale even for those impervious sites difficult to reach.

Essential Variables (EV), a key set of measurements, required for monitoring purposes can be retrieved from RS data in the form of indices and indicators used as proxies to assess quantification and mapping of LD.

The relevant effort of NewLife4Drylands project consists in the extraction of those indices and indicators at a local scale, that is the study sites scale, trying to answer to the requests, by local institutional decision-makers, of increasingly more details difficult to reach by global/pan-European Union (EU) services (i.e., Copernicus).

The 6 study sites represent a wide variety of ecosystems in the Mediterranean landscape as drylands, coastal or mountainous, with high or low extension, threatened from different pressures causing LD, as assessed in Deliverable A1.1. Hence, the analysis by RS data results not site-dependent rather specific for Mediterranean ecosystems identifying a proper protocol for the monitoring of their LD status.

The same RS indicators can offer indications for the assessment of the effectiveness of NBS solutions for LD recovery implemented in the study sites both by NewLife4Drylands and other LIFE projects.

"From data to generate knowledge useful for recovery"

represents the common thread during the whole NewLife4Drylands project development.

2. The role of remote sensing in land degradation assessments: opportunities and challenges

For decades now, LD has been identified as one of the most pressing problems facing the planet: it is one of the biggest global challenges for the people's livelihoods and environment all around the world. Moreover, as land degradation directly affects vegetation biophysical processes and leads to changes in ecosystem functioning, it has a knock-on effect on habitats and, therefore, on numerous species of flora and fauna that become endangered or/and extinct (Symeonakis, 2021).

Figure 1 shows examples of sites affected by LD due to different pressures.
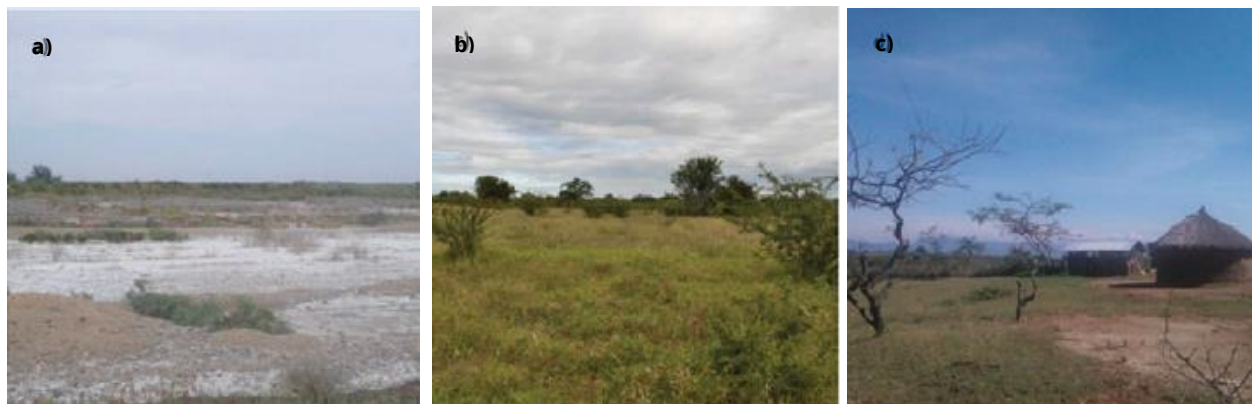
Figure 1. Examples of degraded land: (a) Highly saline degraded cropland in Khorezm Region of Uzbekistan; (b) Bush encroachment in communal land in Limpopo Province of South Africa; (c) Land degradation due to overgrazing in West Pokot County of Kenya (Dubovyk, 2017).

The concerns of the world community about this issue resulted in the proclamation of the United Nations Convention to Combat Desertification (UNCCD) in 1994 (http://www.unccd.int/) which aims at a reduction of LD processes and desertification in all affected countries (Dubovyk, 2017). Specifically the term desertification differs from LD in the different semantic meaning. Indeed degradation of land is caused by various factors including desertification, climatic variations and human-induced activities. The definition by UNCCD refers to LD as the "reduction or loss of the biological or economic productivity and complexity of rainfed cropland, irrigated cropland, or range, pasture, forest and woodlands

resulting from land uses or from a process or combination of processes, including processes arising from human activities and habitation patterns" (UNCCD, § 5, 1994).

The processes commonly identified as the driving factors behind LD are both biophysical/climatic (e.g. steep slopes; soil erosion by water or wind; soil salinization; natural hazards; bush encroachment; alien species invasion; drought; extreme climate events) as well as anthropogenic (land use/cover change as agricultural expansion or abandonment, deforestation, urbanisation, grazing intensification, fuel wood extraction and unsustainable land management practices) including policies, institutions and other socio-economic factors (Nkonya et al., 2011). Local policies and institutions, indeed, have a large impact on sustainability of land management practices, and thus, could either have a direct or indirect impact on behaviour of land users.

Therefore, LD itself is a complicated area of research due to its interdisciplinary nature incorporating geographical, ecological, climatic and social perspectives (Vogt et al., 2011). This complexity partly arises due to an on-going discussion on the definition of what actually constitutes degradation and how it should be measured (Reynolds et al., 2011).

During the last decade, the most widely used approach in assessing LD has been to employ Earth Observation (EO) data in situ or remote sensed. RS is a discipline that employs theories and methods related to extraction of information about surfaces through the interaction of electromagnetic radiation with matter (Li et al., 2009). It is the acquiring of information at a certain distance from a target detecting and recording reflected or emitted energy. Since the launch of the first EO satellites in 1970s, satellite RS has been representing an unprecedented opportunity for people to observe their planet from space.

RS can offer more potentialities as:

1) collecting the signal from the investigated target within a wide range of wavelengths, not only in the visible spectrum, highlighting properties of matter invisible to the human eye;

2) acquiring repeated series imagery of the same scene in order to capture changes over time;

3) analysing phenomena at different spatial scales of detail and investigating even inaccessible areas that are difficult to reach by expensive in-situ explorations.

RS can see no more than human eyes but rather better through integration of spatial, temporal and spectral information. Currently, RS data are featured by satellite multi-platforms, multi-sensors and multi-scale sensors' capabilities covering a wide spectrum of electromagnetic radiation characterized by a range of temporal, spatial and spectral resolutions that are used for various applications in different domains. These observations allow for past, present and near-real-time monitoring of Earth processes (Li et al., 2009). The data archives from the EO sensors allow retrospective analyses of the state and development of land on different spatial scales. Satellite imagery confirms to the principles of repetitiveness, objectivity and consistency, which are preconditions in the framework of LD monitoring. Among different methods and techniques for studying and monitoring LD, RS provides a cost-effective evaluation, back in time, over extensive areas even for those impervious areas difficult to reach, whereas in-situ process studies are time-consuming, resource demanding, and thus, are usually conducted at a field level (e.g., Bai &Dent, 2009; Prince et al. 2007; Gao & Liu, 2010; Vlek, Le, & Tamene, 2008). Furthermore, by using artificial intelligence algorithms trained with few ground truth samples, information where we do not have any can be obtained.

In addition, satellite-based assessment is currently the only means for LD monitoring at different spatial and temporal scales in a spatially explicit and continuous manner, specifically in the less developed countries where funds for sustainable land management programs are often limited (Sivakumar and Stefanski, 2007). Increased access to satellite imagery and constant development of analytical techniques are stepping up monitoring processes at various spatial and temporal scales. Indeed, working with satellite images has changed severely with the recent advent of free and open High Resolution (HR) data from multi-spectral sensors acquiring in the optical spectrum as Landsat (NASA-USGS portal) and Sentinels constellation (Copernicus-EU Program services). Specifically, Sentinel-2 twins satellites (2A/2B) with their dense time series and high acquisition frequency result a game

changer and is becoming the Gold Standard for vegetation monitoring. Such satellite imagery with high spatial and temporal resolutions, offering spectral information in the Vis/NIR, SWIR and RedEdge, increase significantly the amount of essential information allowing monitoring of landscape changes at different scales and planning for more efficient mitigation measures.

Figures 2 and 3 show the main information about Landsat and Sentinel-2 missions compared.

Main Information	Landsat	Sentinel-2
Provider	NASA & USGS	ESA
Spatial resolution	30 m	10-20 m
Spectral resolution	multi-spectral (Visible-NIR-SWIR)	multi-spectral (Visible-RedEdge-NIR-SWIR)
Revisiting time	16 days	5 days (tandem configuration)
Availability time-series archive	since 1972	since 2015

Figure 2. Landsat and Sentinel-2 missions main information

Comparison of Landsat 7 and 8 bands with Sentinel-2
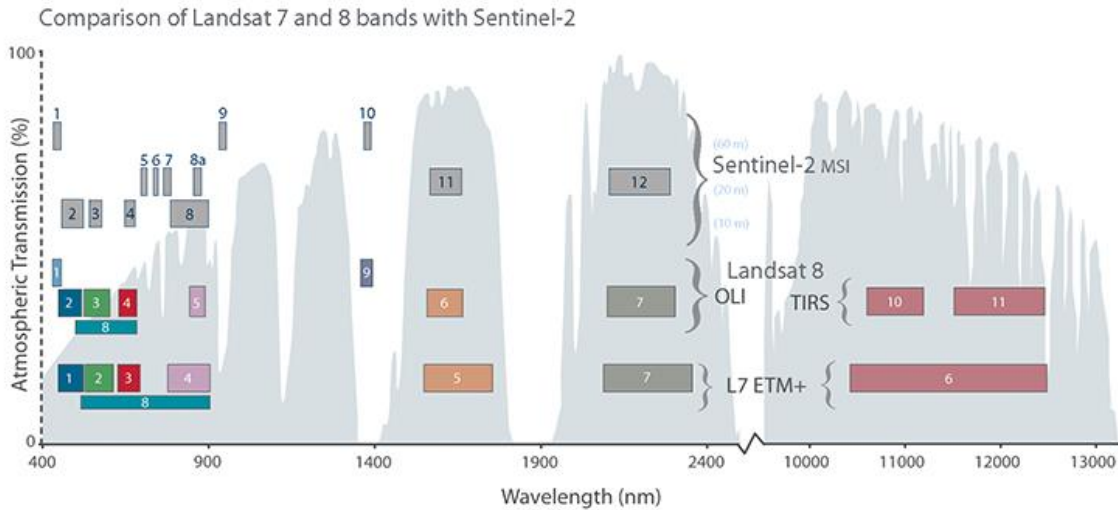
Landsat 8 OLI			Sentinel-2 MSI		
Band	Wavelength range (nm)	Resolution (m)	Band	Wavelength range (nm)	Resolution (m)
1 Coastal aerosol	433 - 453	30	1 Coastal aerosol	433 - 453	60
2 Blue (B)	450 - 515	30	2 Blue (B)	458 - 523	10
3 Green (G)	525 - 600	30	3 Green (G)	543 - 578	10
4 Red (R)	630 - 680	30	4 Red (R)	650 - 680	10
			5 Red edge 1 (RE1)	698 - 713	20
			6 Red edge 2 (RE2)	733 - 748	20
			7 Red edge 3 (RE3)	773 - 793	20
5 Near infrared (NIR)	845 - 885	30	8 Near infrared (NIR)	785 - 900	10
			8a Near infrared narrow (NIRn)	855 - 875	20
			9 Water vapour	935 - 955	60
9 Shortwave infrared / Cirrus	1360 - 1390	30	10 Shortwave infrared / Cirrus	1360 - 1390	60
6 Shortwave infrared 1 (SWIR1)	1560 - 1660	30	11 Shortwave infrared 1 (SWIR1)	1565 - 1655	20
7 Shortwave infrared 2 (SWIR2)	2100 - 2300	30	12 Shortwave infrared 2 (SWIR2)	2100 - 2280	20
8 Panchromatic	500 - 680	15			

Figure 3. Landsat and Sentinel-2 missions spectral bands and wavelengths. To date Landsat 7 and 8 continue to acquire data.

In the use of optical satellite (passive sensor) data a crucial issue is represented by the presence of cloud cover and related shadow which can affect data in addition to the constraint of the sun presence. This issue results in a limited number of available/usable archive scenes. Indeed active sensors, as Synthetic Aperture Radar (SAR) on board of Sentinel-1, can acquire even with cloud coverage but the signal contains information related to moisture content or surface roughness of the investigated area rather than to the optical properties. In addition SAR data require a more complex data handling.

In particular, indicators, extracted from RS data, that address soil condition and vegetation status, represent a high potential in improving desertification assessment at local level, supporting ecological restoration through NBS. Of course, there is a strong need for relevant ground-based information, not only to ensure proper design of NBS but also as a key in-situ data for the proper calibration of satellite imagery analysis and validation of derived products.

Thanks to the technological advancements and the computational capacity of computers on the one hand, together with the availability of open-access remotely-sensed data archives on the other, remote sensors, providing a global perspective and a wealth of data about Earth systems, enable data-informed decision making based on the current state of our planet for its future planning.

Remote Sensing role results in the assessments of the different levels of LD that is mapping of its extent, types and severity at different spatial scales. The spectral, spatial and temporal resolution of these studies varies considerably, and multiscale, multitemporal and multisensor approaches have evolved. Among different Remote Sensing methods developed for LD studies, analysis of <u>vegetation cover dynamics</u> and <u>vegetation productivity and cover decline</u> analysis are the most commonly applied.

Vegetation cover dynamics: Changes and modifications of vegetated land surfaces, such as habitat loss and LD, are regarded as the primary cause for global environmental change as they reduce ecosystem services and impair ecosystem function (Gillanders et al., 2008). Vegetation cover results an indicator of vegetation responses to environmental factors including rainfall, temperature, soil and topography, as well as factors related to human activities, which are typically derived from Land Cover/Land Use (LCLU) information (e.g., irrigated agriculture). Linking vegetation cover dynamics with climatic and anthropogenic factors facilitates an improved understanding of vegetation cover changes as well as ecosystem's feedbacks to natural stresses (e.g., droughts) and human activities (Brown et al., 2010). Moreover, some changes in LCLU are sometimes regarded as LD-enabling factors (i.e., deforestation or encroachment of invasive species). Several systematic techniques were

developed to perform vegetation dynamics analysis and change detection using satellite images (time series or multi-temporal images).

The evolution of the RS-based methods for LD mapping, monitoring and assessment is summarized in Table 1 (Dubovyk, 2017) .

Table 1. The evolution of RS data and methods used for LD assessment.

	1970–1980	1980–1990	1990–2000	2000–2010+
Input data	Multi-spectral images, aerial photos	Multi-spectral images, aerial photos and derivatives, vegetation indices	Multi-spectral images, aerial photos and derivatives, vegetation indices, derivatives from spectral transformation (Tasseled cap, PCA, SMA), vegetation biophysical parameters	UAV images and aerial photos (and derivatives), multi- and hyper-spectral image (and derivatives) time series, vegetation indices and vegetation productivity estimates, yield estimates, spectral transformation, vegetation biophysical parameters,
Methods (examples)	Visual interpretation of aerial photos, photo-grammetric methods, manual mapping	Image classification, map digitalization, expert mapping, photo-grammetric methods, manual mapping	Image classification, spectral transformation, change detection, semi-quantitative image analysis, expert mapping	Time series analysis, data fusion, LD modeling, image classification, spectral transformation, change detection, participatory mapping methods
Sensors/platforms (examples)	Aerial cameras, CORONA, Landsat MSS	Landsat TM, SPOT, AVHRR	Landsat ETM/ETM+, SPOT, ASTER, AVHRR	Landsat, SPOT, AVHRR, Aster, MODIS, MERIS, Sentinel, RapidEye, IKONOS, Quickbird, GeoEye, Hyperion, UAV
Resolutions (examplary ranges)	1–80 m, panchromatic and few multispectral bands	1 m to 8 km, panchromatic, multispectral and thermal bands	1 m to 8 km, increasing number of bands	0.01 m to 8 km, increasing number of bands, hyperspectral sensors

PCA: principal component analysis; SMA: spectral mixture analysis; NPP: net primary productivity; AVHRR: Advanced Very High Resolution Radiometer; MODIS: Moderate Resolution Imaging Spectroradiometer; MERIS: Medium Resolution Imaging Spectrometer; Landsat MSS: Multispectral Scanner; Landsat TM: Thematic Mapper; Landsat ETM: Enhanced Thematic Mapper; SPOT: Satellite for Observation of Earth; ASTER: Advanced Spaceborne Thermal Emission and Reflection Radiometer; UAV: unnamed aerial vehicle.

Vegetation productivity and cover decline: LD manifests itself in the reduced productive potential of a particular landscape or land unit (Reynolds et al., 2007). A gradual loss of vegetation productivity and cover over time is often used as a proxy of LD when Remote Sensing is used for its assessment.

Remote Sensing-based analyses of vegetation productivity decline and vegetation cover decline rely on a wide range of change detection methods (Higginbottom & Symeonakis, 2014).

Currently, there are still on-going discussions and unresolved questions related to the use of satellite RS to address LD, including but not limited to methodological issues, which needs to be approached according to each different case study, such as:

- choice of LD proxy when mapping vegetation cover and productivity changes at different spatial/temporal scales (Prince et al., 2007; Tüshaus et al., 2014);

- data/method selection for multi-temporal/multi-spatial analysis (Le et al., 2016; Wessels et al., 2012);

- analysis of the drivers of LD at different spatial/temporal scales (Bai et al., 2008; Reed et al., 2011);

- decoupling environmental signals due to short term climatic variability and land management from long-term resource degradation (Nkonya et al., 2016a; Stavi & Lal, 2015); and

- validation of the RS results against in situ data (Karnieli et al., 2013; Safriel, 2007).

The outlined research needs are due to the complexity of the LD processes which manifest differently across various spatial and temporal scales. Hence, the importance of the multi-scale assessment and analysis of the cross-scale linkages in LD research are recommended (Reed et al., 2011).

Two broad categories of scale can be defined depending on either their relevance with regard to human impacts (farm/household, community, district/provincial and national/international) or their relevance with regard to environmental impacts (patch, local, landscape, regional and global) (Reynolds et al., 2011). The latter corresponds to ecological view on scale, while the former reflects a planning notion to support sustainable land planning and management. Both types of scale are equally important in LD-based assessment.

However, the choice of the relevant scale(s) depends on the study's aims and specific applications. Consequently, there is currently the need of LD assessments and its drivers at different spatial scales and across various ecosystems, which are largely characterized by local specific problems that have to be prioritized. Besides mapping LD patterns, it is equally

important to go one step further and to analyse the drivers of these processes for a correct interpretation of the produced maps of degraded land (McDowell et al., 2015).

Despite the importance of the problem of LD and its acknowledgment at a global level, to date no consensus has been achieved on systematic and standardized approaches that can be utilized for its assessment and monitoring at different spatial scales. Consequently, there is a pressing need to improve (rather than develop new approaches and methods) and to consolidate existing methods, as well as to calibrate them using in-situ data, to obtain accurate measurements for the monitoring of the extent of degradation at multiple spatial scales to satisfy environmental and natural resource management, policy and research needs. There is also a need for further integration of RS-based approaches and data with the existing process-based LD models and socio-economic approaches for LD assessment in order to capture interdisciplinary nature of this phenomenon.

2.1 The spatial and temporal framework

An existing challenge of RS for LD assessment is represented by the mismatch between spatial and temporal resolution of currently available satellite imagery enforcing for a compromise in the choice for the specific satellite data to be used. In Figure 4 the different environmental and human processes linked to LD in relation to the available satellite data, open and commercial, are depicted.
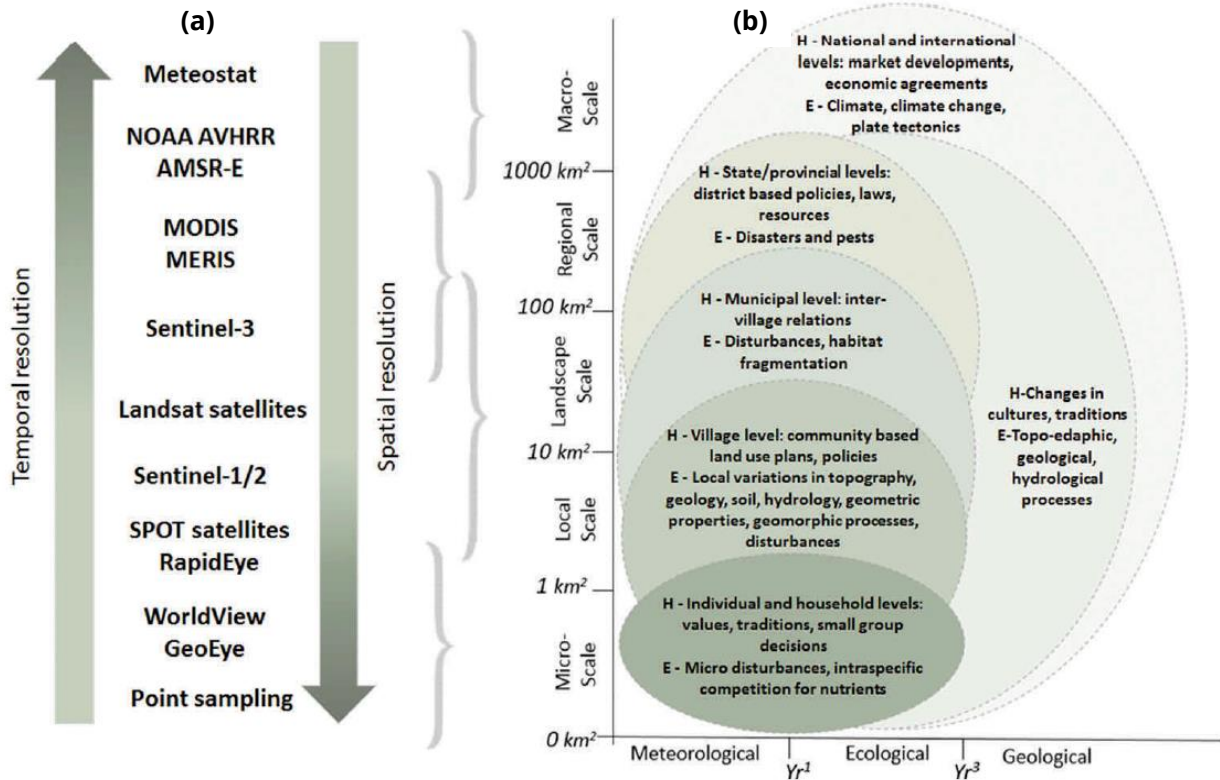
Figure 4. Landsat schematic representation of different spatial and temporal resolution of satellite imagery and their relation to various spatial and temporal scales of environmental and human processes linked to LD: (a) Spatial and temporal resolution of selected satellite imagery; (b) Simplistic representation of hierarchy theory diagram showing that human (H) and environmental (E) processes influence land state (degraded or non-degraded) through land management activities. The indicated scales are not absolute. The listed processes at one specific scale may also occur at other scales. Sub-scales could be identified for each mentioned scale (re-drawn and modified after Buenemann et al., 2011; Dubovyk, 2017).

For mid-long term purposes Landsat archive represents the recommended solution due to the availability of time series imagery back in the past (Figure 2), with acquisitions every 16 days in the Vis/NIR/SWIR of the spectrum but at the lower spatial resolution of 30 meters. Otherwise, for short term or monitoring from 2015 forward purposes Sentinel-2 data represent the solution at the finest spatial resolution of 10-20 meters, with acquisitions every 5 days in the Vis/NIR/SWIR and RedEdge spectrum. Therefore, the choice of the specific satellite data strongly depends on the spatial and temporal framework in which LD is to be analysed. In Figure 5 the same scene acquired at different spatial resolution by Landsat and Sentinel-2 satellites can be appreciated.
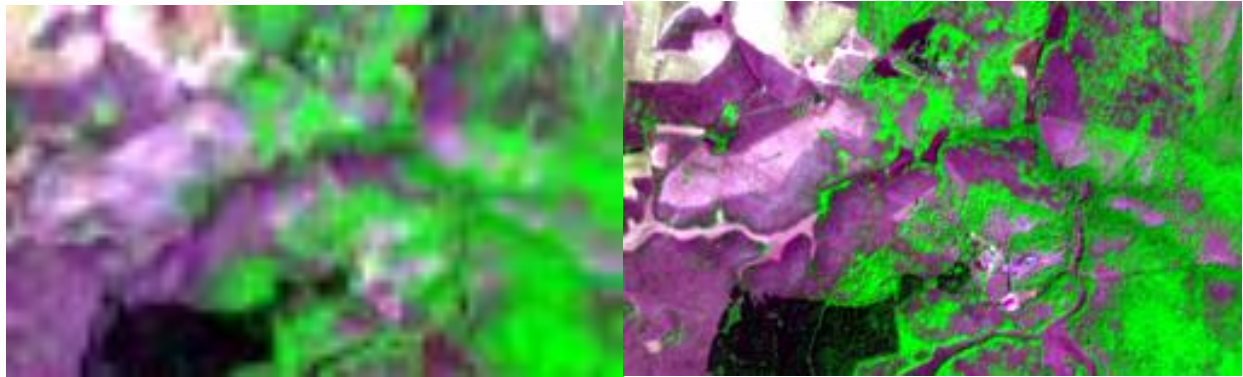
(a)   **(b)**

Figure 5. The same scene acquired from: (a) Landsat at 30 meters; (b) Sentinel-2 at 10 meters.

False colour composite: RGB = NIR-Green-Blue.

Figure 6 shows the different information coming from a multi-temporal acquisition namely the same scene acquired at different time as different seasons can result. By using an intra-annual time series more acquisitions during the same solar year, useful for following the entire cycle of vegetation phenology, are evaluated or with an inter-annual time series composed by more acquisitions during more years, long-term monitoring can be possible. Higher the revisit time of each satellite denser the time series data which will result composed by more images.
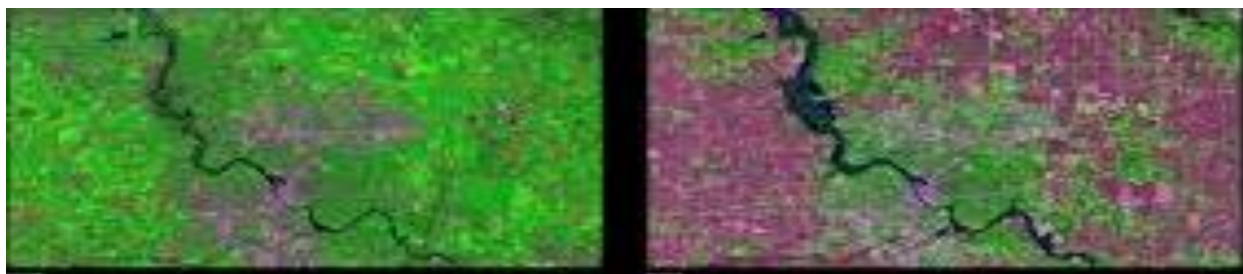
(a)   **(b)**

Figure 6. The same scene acquired on: (a) May (peak of biomass for vegetation); (b) October (senescence for vegetation in pink colour). False colour composite: RGB = NIR-Green-Blue.

2.2 Spectral response of different target

Spectral investigation offers the opportunity to explore properties of matter in a wide range of wavelengths which cannot be observed by human eye to characterise each different target. Figure 7a shows the spectral signal of reflectance from water, soil and vegetation targets: the different reflectance response can be used to differentiate different targets. The typical spectrum of a vegetation target exhibit a low maximum peak in the Green (vegetation appears in green colour) and an highest peak in the NIR, with an upward ramp in the RedEdge and two other lowest peaks in the SWIR portion of the electromagnetic spectrum. The spectrum also varies as the target matter content varies (Figure 7b and 7c).
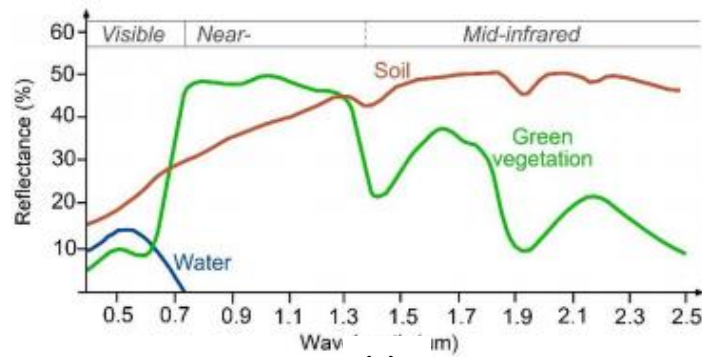
(a)
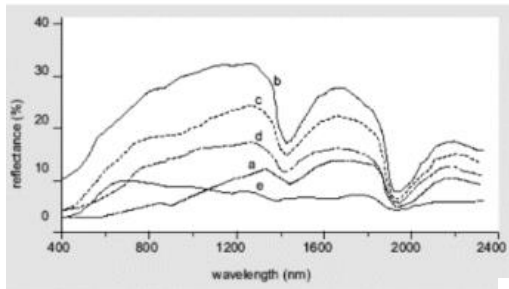
Reflectance spectrum for 5 different soils:
(a) Predominance of organic matter
(b) Traces of different minerals
(c) Traces of iron
(d) Traces of organic matter
(e) Mainly iron

(b)
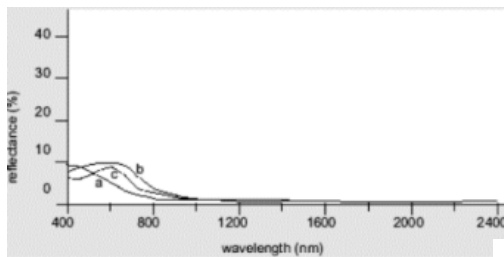
Reflectance spectrum for water with clorophyll and sediments:
(a) Oceanic water
(b) Torbid water
(c) Water with clorophyll

(c)

Figure 7. Reflectance electromagnetic spectra. (a) Different types of targets; (b) Soils with different content; (c) Water with different content.

2.3 Extraction of information from remote sensing data: combination of spectral and temporal domain

RS techniques can exploit the combination of spectral and temporal information provided from satellite imagery considered. In Figure 8 a time-series of a spectral indices (on the left), that is the Normalized Difference Vegetation Index (NDVI), represents the source to extract the phenology profile of a vegetation pattern (on the right). The vegetation cycle can be appreciated by the temporal profile of a traditional spectral index suitable for the study of vegetation.
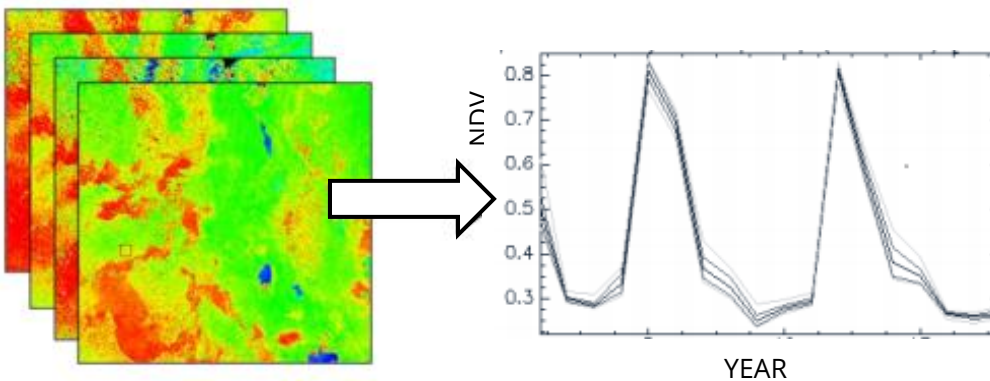
Figure 8. On the left a time series of the NDVI spectral index; on the right the NDVI temporal profile of a vegetation pattern.

2.4 From a global to a local assessment: the working scale

A further challenge of RS for LD assessment is represented by the mismatch between currently available satellite imagery and ecological and socio-economic scales of LD processes and its drivers (Figure 9). For example, to assess LD at a landscape scale, high spatial resolution imagery, such as from Sentinel program, is not always available at frequent and repeatable intervals over long periods in the past that are required for trend analysis. Because of this, no optimal method exists to assess LD at present.

Figure 9 shows clearly differences between geographical, ecological and planning perspective scale and the challenge of finding suitable satellite data sets to perform analysis

at multiple scales. As in the case of scale dependency when mapping degraded areas, the factors that drive vegetation dynamics and degradation are also scale-dependent: for example, gross basal area of pasture is a slow variable at the household scale. At the same time, it is a fast variable at the national scale (Reynolds et al., 2011). Many important issues, therefore, arise from conflicts between scales and a lack of suitable multi-scale data sets needed for analysis, for example, when agricultural policies at national level do not allow for appropriate local management decisions. In a such complex situation, the analyst should be guided by the main scope of the assessment and its application (Dubovyk, 2017).

The estimates derived from coarse resolution satellite data and/or expert opinions are, in general, not suitable for policy-making or for scientific investigations of the potential land rehabilitation measures (Dubovyk et al., 2013a). Moreover, the coarse spatial resolution of global LD maps is not appropriate to support region-based sustainable land use planning, while national maps are not always in place for all countries.

In order to meet the needs of local decision-makers, one of the great challenge of NewLifeforDrylands project is not the searching for new methodologies for LD assessment, but rather to decline on a local scale those well known in the literature. To work at a local scale too low scale ancillary data are not recommended (e.g., Corine Land Cover is produced at 100 meters spatial resolution) because of the too rough detail level at which they are produced which makes them inadequate. Therefore, supported by the experts who know the study areas, the problems of each individual site have been analysed, pressures and threats examined to identify a set of indicators that can be extracted from remote sensing data for the LD assessment. As a result a sort of protocol containing guidelines for the whole procedure has been outlined. The protocol should not be considered a site-specific solution but, rather, it is appropriate for Mediterranean sites hosting different ecosystem types (drylands, coastal, mountainous) each one affected by specific treats.
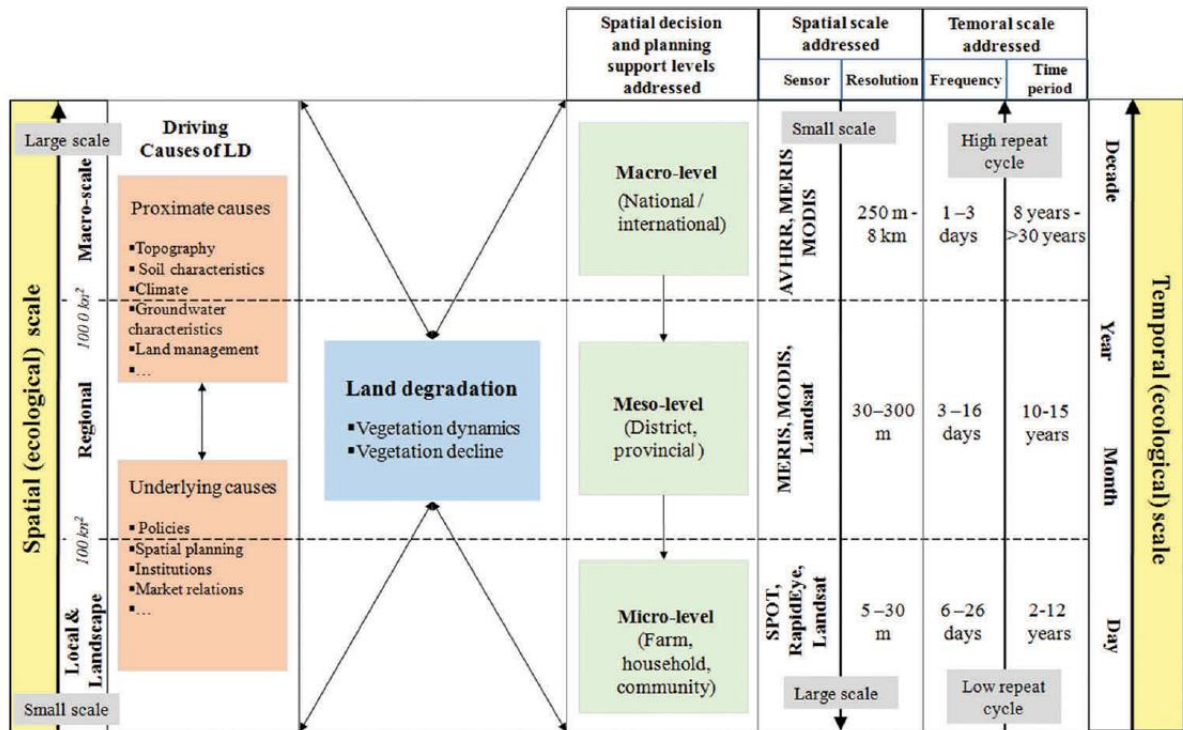
Figure 9. The relationship between ecological scales, spatial and temporal resolution of the exemplary satellite sensors and spatial decision and planning support levels.

The choice of the scale has been made as both extent and grain. The extent has been identified with the boundary of the Natura 2000 Protected Area (PA) within the study site and a buffer area of 5 km around, according to (ISPRA, 2014), to appreciate pressures effects inside and immediately outside the protection level. The grain has been defined according to the level of detail needed for investigation (e.g., at single tree level or at landscape level) that matches with the spatial resolution of satellite data to be considered. Hence, even though a project constraint is in the use of open satellite data, for site of extent less than 50 hectares the need of using Very High Resolution (VHR) commercial satellite data has emerged.

3. Indicators from open satellite data for the evaluation of land degradation

The identification of a set of indicators for the assessment of LD to be extracted from remote sensing data has been carried out based on current scientific and technical literature, consortium members' expertise and discussions with the Advisory Board.

No new research activities can be planned within NewLife4Drylands.

Mainly, the selection provided consists of well-known indicators and the related technical and scientific procedures to generate them from open satellite data. Remote sensing techniques proposed in this project require essential interaction with the fundamental expert knowledge acquired in the field to be used for the training of supervised learning algorithms, calibration of the models and validation of the derived products. The selected indicators come from the list of EVs or their proxies as the spectral indices.

The concept of Essential Variables (EVs) has emerged within the remote sensing community in recent years. The EVs, having previously defined as a minimal set of variables that determines the system's state and development, have attracted considerable interest not only for remote sensing scientists, but from several, diverse thematic groups and communities. The driving forces behind this evolution, relates primary to the need to support national to global monitoring, reporting, research, and forecasting of complex earth systems according to the goals of different thematic communities as well as to the requirement to support consistent, objective temporal information provision for policy development and implementation. So far, EVs have been introduced and adopted for monitoring oceans, climate and biodiversity systems as well as measuring progress towards UN Sustainable Development Goals (SDGs) implementation, while several other communities are in the process of adopting this concept in their domain. Originally, the concept of EVs has been defined by the climate community through the effort led by the Global Climate Observing System (GCOS) which established a set of 52 Essential Climate Variables (ECV) (Giuliani et al., 2020a). The full list can be checked on the GCOS website (https://gcos.wmo.int/en/essential-

climate-variables). Belong to this list LC, Leaf Area Index (LAI), Soil Carbon, Fire, Soil Moisture to name a few.

Table 2 and 3 show the list of spectral indices and indicators from RS data, respectively, identified for NewLife4Drylands project purposes. The former is organized by the different target addressed (i.e., vegetation, soil, water etc.). The generic formula for each index/indicator has been deduced for Sentinel-2 spectral bands and the degradation process that can be investigated has been reported too. This is not an exhaustive list but just a selection of the main well-assessed spectral indices and indicators which could be useful for the project purposes.

Moreover, Table 3 shows, for SDG 15.3.1 indicator (SDG 15.3.1, 2021) the series of further sub-indicators suggested by (Assennato et al., 2020). According to (Assennato et al., 2020), for an effective analysis of LD at local level, NewLife4Drylands project focuses on the need to consider additional sub-indicators suitable for taking into account, at a local scale, pressures and threats which affect the specific study area causing LD. Indeed, UNCCD recommends (but does not prescribe) that SDG 15.3.1 indicator should be complemented by other relevant national (or sub-national) indicators (Wunder and Bodle,2019). Therefore, the list of indicators in Table 3 is not exhaustive but it needs to be rearranged for each study site.

Table 2. Spectral Indices from RS data useful for LD assessment: generic formulas adapted to Sentinel-2 bands and the LD process they can investigate are reported. R is the reflectance at the central wavelengths (nm) denoted by the subscripts.

Type	Name	Formula	Formula by Sentinel-2 bands	Reference	By RS data	Degradation process in the study sites
Vegetation Indices	NDVI Normalized Difference Vegetation Index	$\dfrac{R_{800} - R_{670}}{R_{800} + R_{670}}$	$\dfrac{NIR - Red}{NIR + Red}$	Rouse et al. (1974); Zarco-Tejada et al. (2001)	Yes	Decline in Biodiversity; Decline in Biomass; Decline in vegetation community functioning; Decline in vegetation cover
	GNDVI Green Normalized Difference Vegetation Index	$\dfrac{R_{800} - R_{550}}{R_{800} + R_{550}}$	$\dfrac{NIR - Green}{NIR + Green}$	Gitelson et al. (1996)		
	MSAVI$_2$ Modified Soil-Adjusted Vegetation Index	$\dfrac{2R_{800} + 1 - \sqrt{(2R_{800}+1)^2 - 8(R_{800}-R_{670})}}{2}$	$\dfrac{2*NIR + 1 - \sqrt{(2*NIR+1)^2 - 8*(NIR-Red)}}{2}$	Qi et al. (1994)		
	OSAVI Optimized Soil-Adjusted Vegetation Index	$(1 + 0.16)\dfrac{R_{800} - R_{670}}{R_{800} + R_{670} + 0.16}$	$(1 + 0.16)\dfrac{NIR - Red}{NIR + Red + 0.16}$	Rondeaux et al. (1996)		
	NDRE Normalized Difference Red-Edge	$\dfrac{R_{860} - R_{700}}{R_{860} + R_{700}}$	$\dfrac{NIR_{narrow} - RedEdge1}{NIR_{narrow} + RedEdge1}$	Zhang et al. (2019)		
	ARVI Atmospherically Resistant Vegetation Index	$\dfrac{R_{800} - [R_{670} - (R_{450} - R_{670})]}{R_{800} + [R_{670} - (R_{450} - R_{670})]}$	$\dfrac{NIR - [Red - (Blue - Red)]}{NIR + [Red - (Blue - Red)]}$	Bannari et al. (1995)		
	EVI$_2$	$2.5\dfrac{R_{800} - R_{670}}{R_{800} + 2.4R_{670} + 1}$	$2.5\dfrac{NIR - Red}{NIR + 2.4Red + 1}$	Jiang et al. (2008)		

	Enhanced Vegetation Index2					
	REP **RedEdge Position**	$705+35\dfrac{\left(\frac{R_{670}+R_{780}}{2}\right)-R_{700}}{R_{740}+R_{700}}$	$705+35\dfrac{\left(\frac{\text{Red}+\text{RedEdge3}}{2}\right)-\text{RedEdge1}}{\text{RedEdge2}+\text{RedEdge1}}$	Main et al. (2011)		
	NDMI **Normalized Difference Moisture Index**	$\dfrac{R_{860}-R_{1650}}{R_{860}+R_{1650}}$	$\dfrac{NIR_{narrow}-SWIR1}{NIR_{narrow}+SWIR1}$	Lastovicka et al., (2020)	Yes by proxies from RS	
	PRI **Photochemical Reflectance Index**	$\dfrac{R_{531}-R_{570}}{R_{531}+R_{570}}$	$\dfrac{Blue-Green}{Blue+Green}$ Blue band is too large for accurate estimations	Gamon et al., (1992)	Yes	Decline in productivity
	LAI **Leaf Area Index**	SNAP ESA tool - derived product		https://step.esa.int/main/toolboxes/snap		
Water Indices	**NDWI$_1$** **Normalized Difference Water Index 1**	$\dfrac{R_{800}-R_{2130}}{R_{800}+R_{2130}}$	$\dfrac{NIR-SWIR2}{NIR+SWIR2}$	Gao, 1996; Chen et al., 2005	Yes	Decline in vegetation
	NDWI$_2$ **Normalized Difference Water Index 2**	$\dfrac{R_{550}-R_{800}}{R_{550}+R_{800}}$	$\dfrac{Green-NIR}{Green+NIR}$	McFeeters (1996)		Hydrological modifications
	MNDWI **Modified Normalized Difference Water Index**	$\dfrac{R_{550}-R_{2130}}{R_{550}+R_{2130}}$	$\dfrac{Green-SWIR2}{Green+SWIR2}$	Xu (2006)		
Soil Indices	**NDSI** **Normalized Difference Soil Index**	$\dfrac{R_{1650}-R_{560}}{R_{1650}+R_{560}}$	$\dfrac{SWIR1-Green}{SWIR1+Green}$	Deng et al. (2015); Vibhute et al., 2017	Yes	Soil quality degradation

	NDBSI **Normalized Difference Bare Soil Index**	$\dfrac{R_{1650} - R_{860}}{R_{1650} + R_{860} + 0.001}$	$\dfrac{SWIR1 - NIRnarrow}{SWIR1 + NIRnarrow + 0.001}$	Chen et al. (2004)			
	BI **Bare Index**	$\dfrac{(R_{1650} + R_{670}) - (R_{800} + R_{450})}{(R_{1650} + R_{670}) + (R_{800} + R_{450})}$	$\dfrac{(SWIR1 + Red) - (NIR + Blue)}{(SWIR1 + Red) + (NIR + Blue)}$				
Burned Areas Indices	**NBR** **Normalized Burn Ratio**	$\dfrac{R_{860} - R_{2200}}{R_{860} + R_{2200}}$	$\dfrac{NIR_{narrow} - SWIR2}{NIR_{narrow} + SWIR2}$	Key et al. (2002)	Yes	Forest fires	
	NBR$_2$ **Normalized Burn Ratio 2**	$\dfrac{R_{1600} - R_{2200}}{R_{1600} + R_{2200}}$	$\dfrac{SWIR1 - SWIR2}{SWIR1 + SWIR2}$				
Soil Salinity Indices	**SSI$_1$** **Soil Salinity Index-2**	$\sqrt{R_{[520:600]} * R_{[630:690]}}$	$\sqrt{Green * Red}$	Douaoui et al. (2006); Khan et al. (2001);- Yahiaoui et al. (2015)	Yes	Soil Salinization	
	SSI$_2$ **Soil Salinity Index-2**	$2 * R_{[520:600]}\text{-}(R_{[630:690]} + R_{[770:900]})$	$2 * Green\text{-}(Red + NIR)$	Douaoui and Lepinard (2010); Yahiaoui et al. (2015)			
	SSI$_3$ **Soil Salinity Index-1**	$\sqrt{R^2_{[630:690]} + R^2_{[520:600]}}$	$\sqrt{Red^2 + Green^2}$	Douaoui et al. (2006); Yahiaoui et al. (2015)			
	SI **Soil Salinity**	$\dfrac{R_{[530:590]} * R_{[640:670]}}{R_{[450:510]}}$	$\dfrac{Green * Red}{Blue}$	Elhag et al. (2016)			

	SASI **Soil Adjusted Salinity Index**	$\dfrac{R_{[630:690]}}{100 * R^2_{[450:520]}}$	$\dfrac{Red}{100 * Blue^2}$	Yahiaoui et al. (2015)			
Drought/ Dryness Indices	**NDDI** **Normalized Difference Drought Index**	$\dfrac{NDVI - NDWI_1}{NDVI + NDWI_1}$		Gu et al. (2007); Renza et al. (2010)	Yes	Aridification	
	DSI **Desertification Soil Index**	$\dfrac{R_{1648} - R_{498}}{R_{1648} - R_{2203} + 0.2}$	$\dfrac{SWIR1 - Blue}{SWIR1 - SWIR2 + 0.2}$	Wu et al. (2010)			

Table 3. Indicators and their metric/measure useful for LD assessment: the LD process they can investigate are reported.

Indicator	Sub-Indicator	Metric/Measure	Final Formula for sub-indicators	Reference	By RS data	Degradation process in the study sites
SDG 15.3.1 proportion of land that is degraded over total land area	LC change (Trend in LC)	LC Area	*One Out, All Out*	UNCCD (2017; 2018; 2021); https://unstats.un.org/sdgs/metadata/files/Metadata-15-03-01.pdf	Yes	Habitat loss; Decline in productivity; Trees encroachment; Urban expansion ......
	Land Productivity loss	Net Primary Production (NPP)			Yes by proxies from RS	
	Soil Organic Carbon (SOC) decline	SOC				
	Further sub-indicators					
	Loss of habitat quality	Habitat cover Area	*One Out, All Out*	Assennato et al., 2020	RS (LC/habitat map)+InVEST model	
	Burnt Areas	LC Area			Yes	
	Fragmentation Index	Mesh density			RS (LC)+spatial rules	
	Areas of potential impact	LC Area			RS (LC)+spatial rules	
	Density of artificial LC	LC Density			Yes	
	Increasing of not sealed areas	LC Area			RS (LC)+spatial rules	
	TO BE CONTINUED......					

SDG 15.1.2 Proportion of important sites for terrestrial and freshwater biodiversity that are covered by protected areas, by ecosystem type	Ecosystem within protected area	LC/Habitat Area	$$\frac{\textit{Coverage of an ecosystem within protected area}}{\textit{Coverage of the Key Biodiversity Areas}}$$	https://www.landportal.org/book/dataset/un-sdg1512	Yes	Conservation, restoration and sustainable use of ecosystems
	Key Biodiversity Areas (KBA)	World Database of Key Biodiversity Areas		https://www.iucn.org/resources/conservation-tools/world-database-of-key-biodiversity-areas		
SDG 11.3.1 Ratio of land consumption rate to population growth rate	Land Consumption Rate	$$\frac{\ln\left(Urb_{grid,\,t+n}/Urb_{grid,t}\right)}{n}$$ $Urb_{grid,t+n}$ = surface occupied by urban areas, in the output cell considered, at the final year (t+n).........	$$\frac{\textit{Land Consumption Rate}}{\textit{Population Growth Rate}}$$	https://unstats.un.org/sdgs/metadata/files/Metadata-11-03-01.pdf; Aquilino et al. (2020)	Yes	Urban expansion
	Population Growth Rate	$$\frac{\ln\left(P_{grid,t+n}/P_{grid,t}\right)}{n}$$ $P_{grid,t+n}$ = population living in urban areas, in the output cell			No	

		considered, at the final year (t+n)........				
ESA(I) Environmentally Sensitive Areas to Desertification (Index)	**Soil Quality Index (SQI)**	(Soil Texture $*$ Rock Fragment $*$ Soil Depth $*$ Parent Material $*$ Drainage $*$ Slope Gradient)$^{1/6}$	$(SQI * CQI * VQI * MQI)^{\frac{1}{4}}$	Tsemelis et al. (2018)	RS (slope)+ Ancillary data	Desertification
	Climate Quality Index (CQI)	(Rainfall $*$ Aridity Index $*$ Slope Aspect)$^{1/3}$			RS (slope)+ Meteo data	
	Vegetation Quality Index (VQI)	(Fire Risk $*$ Erosion Protection $*$ Drought Resistance $*$ Plant Cover)$^{1/4}$			RS (vegetation cover; burned areas)+ Ancillary data	
	Management Quality Index (MQI)	(Land Use Intensity $*$ Policy)$^{1/2}$			RS (LC)+ Ancillary data	
SDVI Standardized Drought Vulnerability Index	**cSPI6**	Meteoreological - Hydrological - Agricultural Drought Vulnerability (Standard Precipitations over 6 months)	$SDVI = \sum_{i=1}^{N} \dfrac{\text{Scaled Values of the Components}}{\text{Number of Components } (N = 6)}$	Karavitis et al. (2014); Tsemelis et al. (2018)	Meteo data+ Ancillary data	Drought
	cSPI12 (Standard Precipitations)	Meteorological – Hydrol. Drought Vulnerability (Standard Precipitations over 12 weeks)				

					No	
	Supply	Hydrological - Agricultural - Social Drought Vulnerability				
	Demand	Agricultural - Social Drought Vulnerability				
	Impacts	Social Drought Vulnerability				
	Infrastructure	Hydrological - Agricultural - Social Drought Vulnerability				

4.   The UNCCD and the SDG 15.3.1 indicator

As part of the "2030 Agenda for Sustainable Development", the SDG 15.3.1 indicator, "*proportion of land that is degraded over total land area*" (SDG 15.3.1, 2021), has been supported by NewLife4Drylands project for the need to develop a standardized methodology for LD assessment according to the UNCCD guidelines. These latter aim to achieve Land Degradation Neutrality (LDN), defined as "*a state whereby the amount and quality of land resources necessary to support ecosystem functions and services and enhance food security remain stable or increase within specified temporal and spatial scales and ecosystems*" (UNCCD, 2015). Achieving LDN can become an accelerator of achieving SDGs across the board (https://www.unccd.int/issues/land-and-sustainable-development-goals). SDG 15.3.1 indicator, with its three main land-based sub-indicators already monitored in the context of the UNCCD reporting process (UNCCD, 2017; 2018; 2021), results well suited.

SDG 15.3.1 Indicator is calculated as a binary - degraded/not degraded - quantification using three sub-indicators which are:

1. Trends in LC (LC change): as vegetation cover to assess land conversion trends and the possible loss of ecosystem services;
2. Trends in land productivity (NPP): to determine changes in health and capacity of primary production;
3. Trends in carbon stocks (above and below ground), currently represented by SOC stocks: to quantify overall soil quality

The above-mentioned three sub-indicators, proposed to measure the SDG 15.3, underline the importance of spatiotemporal monitoring of land cover dynamics and land productivity for LD assessments. In this light, the role of EO and specifically RS data, has gained unpredictable importance.

Essentially, any significant reduction or negative change in one of the three sub-indicators is considered to comprise land degradation.

To extract the mentioned trends a temporal baseline needs to be established. The *one-out, all-out* principle is used to evaluate the sub-indicators and determine LDN status. According

to this principle, LD occurs when, compared with the temporal baseline (https://knowledge.unccd.int/ldn/ldn-monitoring):

1. Negative land cover change occurs (loss of a specific LC class) or

2. NPP decrease significantly or

3. SOC decrease significantly.

As such, the sub-indicators are quantified and evaluated separately. As gains in one of these measures cannot compensate for losses in another, if one of the sub-indicators shows a negative change, LDN is not achieved, even if the others are substantially positive.

The detailed methodology is shown in Figure 10.
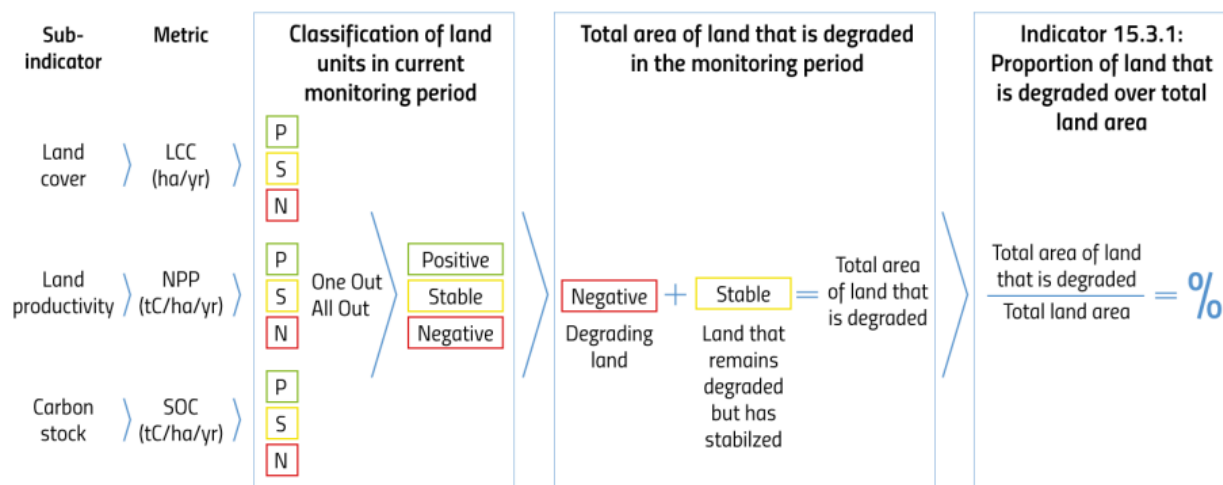
Figure 10. Combination of the three sub-indicators to define SDG15.3.1 indicator value.

Figure 11 provides a simplified example about how LDN is monitored using the sub-indicators to identify areas of change and how the *one-out, all-out* principle to identify gains and losses can be applied.

The baseline values for each land unit (A1-A5) are "t0" and "t1". Gains and losses, in terms of land area, are to be considered for each land unit (A1-A5) and then summed to determine the LDN status (net gain) for that LC type (grassland in the example shown).

A Map of Land Types (Land Type "A" = Grassland)	Context*	Metric values at Baseline (t0)	Decisions	Metric values in Future (t1)	Gains vs. Losses (t1 - t0)
	A1 Land Area: 15,000 ha Use: short grazing period Status: Not Degraded	Land Cover: Grassland NPP=11.7 tDM/ha/yr SOC=54.5 tC/ha	Grazing period extended	⊘ Land Cover: Grassland ↓ NPP=7.1 tDM/ha/yr ⊘ SOC=53.9 tC/ha	**Loss:** 15,000 ha significant degradation
	A2 Land Area: 25,000 ha Use: grazing excluded Status: Not Degraded	Land Cover: Grassland NPP=12.8 tDM/ha/yr SOC=63.6 tC/ha	Livestock exclusion maintained	⊘ Land Cover: Grassland ⊘ NPP=13.1 tDM/ha/yr ⊘ SOC=63.8 tC/ha	**No Change In LDN Status** 25,000 ha stable
	A3 Land Area: 10,000 ha Use: long grazing period Status: Degraded	Land Cover: Grassland NPP=6.5 tDM/ha/yr SOC=51.1 tC/ha	Long grazing period continued	⊘ Land Cover: Grassland ↓ NPP=3.9 tDM/ha/yr ↓ SOC=40.7 tC/ha	**Loss:** 10,000 ha significant degradation
	A4 Land Area: 40,000 ha Use: med. grazing period Status: Degraded	Land Cover: Grassland NPP=10.3 tDM/ha/yr SOC=47.6 tC/ha	Sustainable grazing management introduced	⊘ Land Cover: Grassland ⊘ NPP=10.8 tDM/ha/yr ↑ SOC=51.2 tC/ha	**Gain:** 40,000 ha significant improvement
	A5 Land Area: 10,000 ha Use: short grazing period Status: Not Degraded	Land Cover: Grassland NPP=11.9 tDM/ha/yr SOC=54.6 tC/ha	Urban expansion	↓ Land Cover: Urban ↓ NPP=7.1 tDM/ha/yr ⊘ SOC=54.3 tC/ha	**Loss:** 10,000 ha significant degradation

Metrics

Land Cover: nationally refined land potential class where change in class may be characterized as positive or negative

NPP: Net Primary Productivity
SOC: Soil Organic Carbon
DM: dry matter

NPP level (tDM/ha/yr, where a change in the absolute value may be positive or negative

SOC stock (tC/ha, to 30 cm) where a change in the absolute value may be positive or negative

↓ ↓

Land Degradation Neutrality Status (t1-t0): Net Gain: 5,000 ha

Legend

⊘ No significant change in the metric
↑ Significant positive change in the metric
↓ Significant negative change in the metric

● Stable (no change)
● Degraded land or negative change
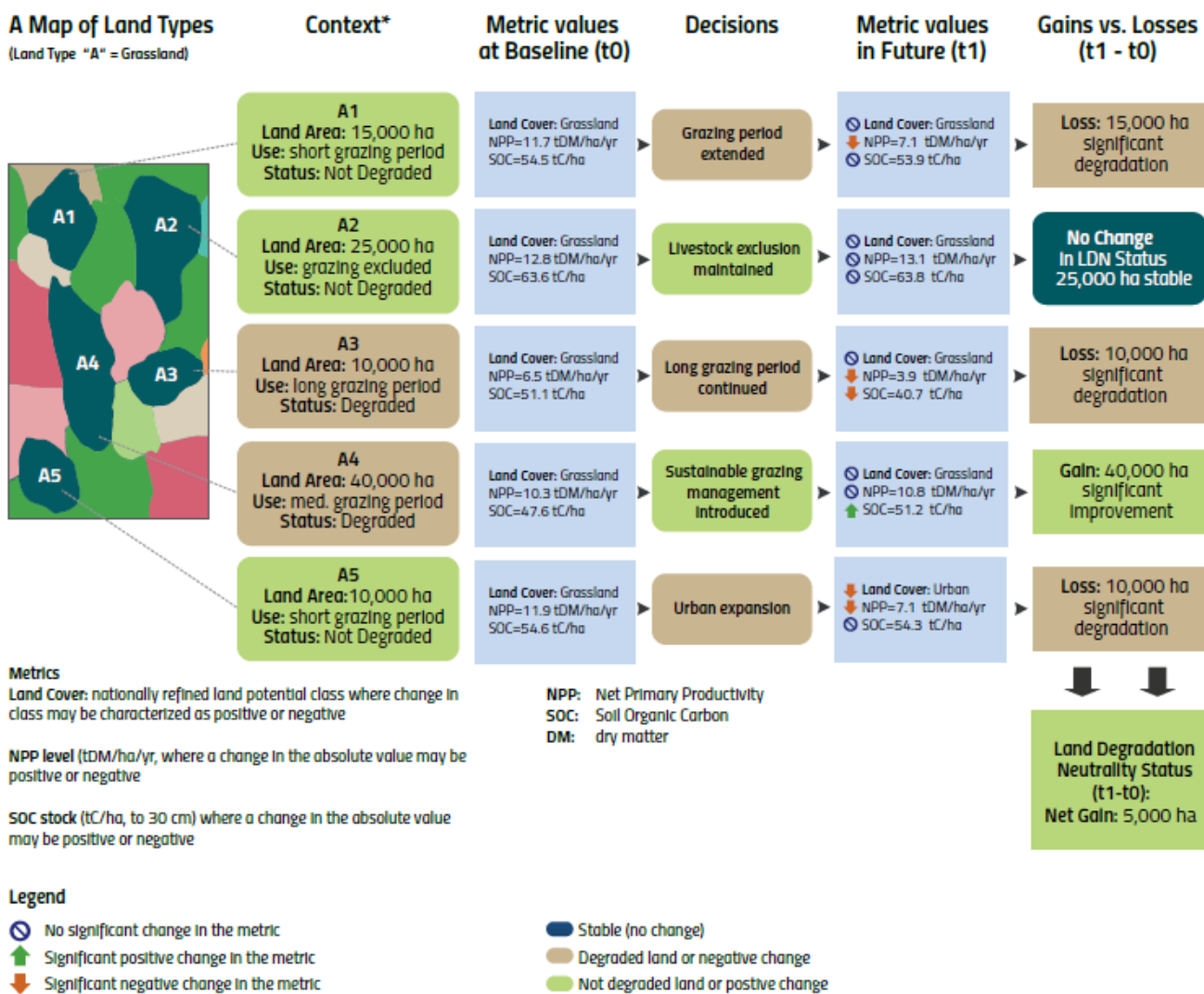● Not degraded land or positive change

Figure 11. An example of application of one-out, all-out principle to combine the three sub-indicators within SDG 15.3.1 indicator for assessing LDN.

The UNCCD is the custodian agency for SDG indicator 15.3.1. Information on this indicator has been regularly collected by the UNCCD through its national reporting and review process since 2018, and every four years thereafter.

At present, SDG 15.3.1 indicator has been upgraded to version 2.0, officially released at the end of September 2021 (SDG 15.3.1, 2021).

UNCCD has developed a Good Practice Guidance providing recommendations on how to calculate SDG Indicator 15.3.1. This document provides a brief introduction to SDG Indicator 15.3.1 and describes how each sub-indicator is calculated by (Trends.Earth, 2018), a free and open-source tool licensed under the GNU General Public License, version 2.0 or later. This tool provides access to global free databases and resources and it can be customized with own data (Giuliani et al., 2020b).

To address national or sub-national priorities in the evaluation of LDN monitoring the UNCCD guidelines suggest additional sub-indicators to be considered. According to this aim, one of the challenge of NewLife4Drylands project is represented by the extraction of further sub-indicators at a local scale, performing the most adequate computation technique, for monitoring pressures and threats causing LD in the different study areas.

The temporal baseline to be monitored has been identified considering trigger events in each study site as wildfires, floodings, vegetation diseases, invasive species spreadings etc. choosing a temporal range for investigation before and after those critical events.

It's crucial the availability of ground truth data for the validation of each sub-indicator considering its accuracy with the associated error estimation by which it is produced with the technique adopted.

4.1   Sub-indicator: Land Cover Trend

The available LC Copernicus services as the Pan-European HR layers (https://land.copernicus.eu/pan-european/high-resolution-layers)(e.g., grassland/forest cover etc.) or the new N2K product (https://land.copernicus.eu/local/natura) which supports the monitoring of Natura 2000 sites, even though produced at 10 meters spatial resolution are obtained at a European level reporting a low level of detail not useful for local evaluations and available only at well-defined time (Tarantino et al., 2021).

Such products are usefull as records data but the end users and stakeholders that are responsible for conservation and management need a close to nowcasting datasets as inputs to their daily activities.

A set of LC maps will be produced at local scale, for each study site, by using Sentinel-2 or Landsat satellite data or VHR data in case of areas less than 50 ha. First of all, for each site, LC classes will be identified according to the spatial resolution of satellite data considered. The Food and Agriculture Organisation (FAO) Land Cover Classification System (LCCS), version 2, taxonomy scheme (Di Gregorio & Jansen, 2005), at level 4, will be adopted for its suitability not only to summarise a series of morpho-structural characteristics of the patch under consideration, but also makes it effectiveness in monitoring activities, repeated in space and time, from space according to (Tomaselli et al., 2013; Adamo et al., 2014; 2016). LC maps will be produced by using machine learning algorithms as Neural Network (NN) (Bishop, 1996), Support Vector Machine (SVM) (Vapnik, 1995; 1998), Random Forest (RF) (Gavish et al., 2018) or any other pixel-based supervised classifier as Convolutional Neural Network (CNN) (Fazzini et al., 2021) from deep learning approach. By using VHR data object-based algorithms will be considered either with a data-driven or knowledge-driven (rule-based) approach.

The series of LC maps will be compared to identify the temporal trend in the presence of each LC class prone to causing LD. From-to class transitions for changed areas will be identified by Post Classification Comparison (PCC) as change detection technique.

To detect changed areas, for those target classes whose presence has been reduced in the scene, the Cross Correlation Analysis (CCA) algorithm can be considered for each class at a time (Tarantino et al., 2016 a; 2016 b).

An essential issue is represented by the need for ground truth data to be available for:

1. Training of the data-driven supervised classification algorithms
2. Validation of the mappings accuracy and associated error

4.2   Sub-indicator: Primary Productivity Trend

The primary production regulates energy, water and nutrient flows in land ecosystems, sequestrates carbon dioxide, and it is the basis of food production and generally provides habitats for species (MEA, 2005). Productivity is a term denoting the growth of vegetation,

often described as Gross Primary Productivity (GPP), which is the growth due to photosynthesis, or NPP, which is the GPP minus the respiration of the vegetation, thus net vegetation growth.

Recently Copernicus services have been enriched with HR Vegetation Phenology and Productivity (HR-VPP) layers within Pan European Biophysical parameters (https://land.copernicus.eu/pan-european/biophysical-parameters/high-resolution-vegetation-phenology-and-productivity). The product has a 10 meters spatial resolution that is adequate for our goal. But we are worried of some potential shortcoming outlined in the "HR-VPP Calibration Report, Issue 1.7" that underline the methodology was set up in northern and central Europe (Tian et al 2021). It was shown the limit in pixel with mixed vegetation and bare soil and the correction with Difference Vegetation Indices (DVI) could be not always up to the task. The choice of Plant Phenology Index (PPI) as vegetation index was a trade-off choice that work best in boreal evergreen forest. Finally, the interpolator uses as model exponential curve with sharp start and end of season point: this kind of seasonality do not represent well Mediterranean area vegetation in which winter or summer low season have often some levels of productivity. Hence, we will compare this product with time series of vegetation spectral indices (phenology trends) as NDVI or Modified Soil Adjusted Vegetation Index (MSAVI) or Enhanced Vegetation Index (EVI) using as interpolator an harmonic model-based approach (Vicario et al., 2020). The best products compared with ground truth will be considered as proxies for trends in GPP for each study site by using Sentinel-2 or Landsat satellite data.

Furthermore Sentinel-2 data will be used for LAI estimations which area correlated to evapotranspiration that can be considered as a proxy for PP (Luo et al., 2004).

The uptake of solar energy by the plant canopy is often quantified by FAPAR (Fractional Absorbed Photosynthetically Active Radiation). There is an asymptotic relationship between FAPAR and LAI leading to a saturation of FAPAR at high LAI. Therefore, FAPAR is a less useful descriptor than LAI of leaf foliage development at high vegetation density which is not the

case for the study sites of NewLife4Drylands project. Hence, FAPAR estimations from Sentinel-2 data will be derived.

4.3 Sub-indicator: Soil Organic Carbon Trend

Remote sensing is a powerful method for mapping soil properties, such as SOC, a key property of soil quality (Thaler et al., 2019). Multi-source Sentinel-2 and hyperspectral data will be considered for the extraction of SOC trend estimations. The latter data will come from the new Italian hyperspectral PRISMA mission (https://www.asi.it/scienze-della-terra/prisma/) by the Italian Space Agency (ASI) which is able to provide 30 meters spatial resolution images with a very high spectral resolution. These data will be considered for data provision or information integration which can allow soil properties and content discrimination.

Recent literature deals with the possibility of estimating SOC from hyperspectral data by means of multi-variate regression analysis. Several approaches have been used (Viscarra Rossel and Behrens, 2010; Vohland et al., 2011; 2017). These approaches use SOC measurements performed in laboratory on soil samples collected in the field as calibration reference data. Although the availability of information from a large number of bands has made hyperspectral sensors the most suitable tools for remote SOC measurements, the current limited availability of hyperspectral data with adequate spatial resolution is a shortcoming that leads to a poor application of spectroscopic investigation for SOC extraction from satellite data. In order to overcome such a gap, several efforts have recently been made to investigate the possibility of measuring SOC from multi-spectral images (e.g. Sentinel-2, Landsat 8). In (Gholizadeh et al., 2018) SOC measurements from Sentinel-2 were obtained using 10 bands and 18 derived spectral indices; in (Thaler et al., 2019) a new index, the Soil Organic Carbon Index (SOCI) exploiting only the visible bands in VHR images, was implemented. As done with hyperspectral data, the methods adopted in these studies are based on the application of regression models and ground-based measurements.

During the project, in order to provide an estimate of SOC two approaches will be used based on: i) the identification and use of spectral indices from Sentinel-2 and Landsat data; ii) the exploitation of PRISMA entire spectrum characteristics through the application of regression analysis techniques and multi-variate calibration methods.

The different methods for SOC extraction will be considered and compared by evaluating their performances considering two different approaches:

1) application of the multivariate calibration to the entire spectral signature acquired by the sensor;

2) application of the multivariate calibration to a series of spectral features properly selected. The latter approach results necessary due to the high dimensionality of the hyperspectral data. Indeed, one of the main problems related to the use of hyperspectral data is the reduction of redundant information through feature selection procedures to exclude spectral variables that do not contain information. Feature selection will be done through the application of the Leave-One-Out cross-validation procedure, which uses a selection criterion based on the minimization of the error found by comparison with in situ measurements.

A crucial point can be represented by the possibility to extract SOC information by correlating reference data with vegetation indices in case of areas covered by vegetation. Vegetation properties could indirectly provide information on soil properties with that specific land cover (Bhunia et al., 2017).

4.4   Further Sub-indicators

Further sub-indicators can be identified from the expert-knowledge of the responsible for the study sites considering events or unique conditions which affect the area contributing to the LD status.

Those sub-indicators are not necessarily the same for all the study sites.

Therefore, invasive species mappings, habitat change maps, seedlings physiological state, burned areas cover trend, hydroperiod mappings, vegetation suffering estimations,

historical meteo data analysis, historical climatological analysis, soil salinity indices will be obtained by using satellite data.

5. Selection of sub-indicators to assess land degradation in the NewLife4Drylands study sites

The six study sites of NewLife4Drylands project have in common belonging to the Natura 2000 network of protected areas and the location in the Mediterranean landscape. They represent an exhaustive variety of the typical Mediterranean ecosystems.

In Table 4 the study sites are grouped by its own dominant ecosystem type.

Table 4. Six study sites of NewLife4Drylands project grouped by ecosystem type.

Study Site	Location	Ecosystem type	Dominant Ecosystem
Alta Murgia	Southern Italy	Drylands	Grassland
Tifaracas	Gran Canaria, Spain		Shrublands
El Bruc	Catalonia, Spain		Forest
Palo Laziale	Central Italy	Coastal	Forest
Nestos	Greece		Riparian Forest
Asterousia	Greece	Mountain	Shrublands

An accurate analysis of the main pressures and threats which contribute to LD status has been carried on each of the six study sites of NewLife4Drylands project collecting information and reporting them in Table 5.

Moreover, the LD processes as identified have been crossed with the spectral indices and indicators selected in Tables 2 and 3 for the LD assessment and the results are collected in Table 6.

The challenge of NewLife4Drylands project consists in the selection of sub-indicators specific for monitoring LD status in each different study site at local scale: the solution identified is not intended as site-specific but rather Mediterranean sites-specific taking into account the possible ecosystem types. Hence the most adequate computation techniques will be identified for the extraction of sub-indicators, for each site, which will, then, be integrated to obtain the SDG 15.3.1 indicator.

Some areas are currently targeted by other LIFE projects which have executed recovery actions from LD applying NBS solutions (Figure 12). So, the sub-indicators will be used also for monitoring, in the medium-long term, the results of the restoration activities as improvement of sub-indicators and SDG 15.3.1 indicator.

New recovery actions will be deployed in the Alta Murgia study site for the recovery of grassland ecosystem: short-term monitoring will be executed in this case due to the short time of the project.

Figure 12. The six study sites of NewLife4Drylands project with indications of other LIFE projects involved.

Table 5. Main LD processes affecting the study sites.

Study Site	Landscape modification	Aridification	Fires	Hydrological modification	Over grazing	Soil salinization	Soil organic matter decline	Soil erosion by water and wind	Decline in vegetation community functioning	Decline in vegetation cover/biomass	Habitat loss	Increase in invasive species	Trees encroachment
Alta Murgia	X	X	X					X	X	X	X	X	X
Tifaracas		X	X	X	X			X	X	X	X		
El Bruc	X	X	X					X	X	X	X		X
Palo Laziale		X	X						X	X	X		
Nestos	X					X	X				X	X	
Asterousia	X	X	X	X	X	X	X	X	X	X	X		
Tot. LD presence across sites	4	5	5	2	2	2	2	4	5	5	6	2	2

Table 6. Main LD processes affecting the study sites crosses with indices and indicators in Tables 2 and 3, respectively.

Study Site	Landscape modification	Aridification	Forest fires	Hydrological	Over grazing	Soil salinization	Soil organic matte	Soil erosion by water	Decline in vegetation communit	Decline in vegetation	Habitat loss	Increase in invasiv	Trees encroach

				modification			r decline	and wind	y functioning	cover/biomass		e species	men t
NDVI	X		X		X					X	X	X	X	X
GNDVI	X		X		X					X	X	X	X	X
MSAVI$_2$	X		X		X					X	X	X	X	X
OSAVI	X		X		X					X	X	X	X	X
NDRE	X		X		X					X	X	X	X	X
ARVI	X				X					X	X	X	X	X
EVI$_2$	X				X					X	X	X	X	X
REP	X				X					X	X	X	X	X
NDMI	X	X			X					X	X			
PRI					X					X	X			
LAI					X					X	X			
NDWI1	X			X							X			
NDWI2	X			X										
MNDWI	X			X										
NDSI	X	X						X	X	X			X	
NDBSI	X	X						X	X	X			X	
BI	X	X						X	X	X			X	
NBR	X	X	X											
NBR$_2$	X	X	X											
SSI1	X	X							X					

SSI2	X	X				X						
SSI3	X	X				X						
SI	X	X				X						
SASI	X	X				X				X		
NDDI	X	X			X	X	X			X		
DSI	X	X			X	X	X			X		
LC change (LCTrend)	X	X	X		X		X	X	X	X	X	X
Land Productivity loss		X	X		X		X	X	X			
Soil Organic Carbon (SOC) decline		X	X		X	X	X	X				
Loss of habitat quality	X	X	X		X		X	X	X	X	X	X
Burnt Areas	X	X	X					X	X	X		
Fragmentation Index	X		X		X			X	X	X		

Areas of potential impact	X		X		X				X	X	X		
Density of artificial LC	X								X		X		
Increasing of not sealed areas	X								X		X		
Ecosystem within protected area	X		X						X	X	X	X	X
Key Biodiversity Areas (KBA)													
Land Consumption Rate	X		X	X									
Population Growth Rate													
Soil Quality Index (SQI)	X	X	X	X	X	X	X	X					

Climate Quality Index (CQI)		X	X			X		X					
Vegetation Quality Index (VQI)	X	X	X		X				X	X	X	X	X
Management Quality Index (MQI)				X		X							
cSPI6		X	X			X		X					
cSPI12 (Standard Precipitations)		X	X			X		X					
Supply	X	X	X		X					X	X	X	
Demand	X	X	X		X					X	X	X	
Impacts	X	X	X		X					X	X	X	
Infrastruct.	X												

5.1   Alta Murgia (Italy)

The N2K "Alta Murgia" study site is a protected area (IT9120007) located in the Mediterranean basin within the Apulia region, Southern Italy. This is a Site of Community Importance (SCI) and in addition a Special Protection Area (SPA), covering nearly 126000 ha, with a National Park included within since 2004. (Figure 13).
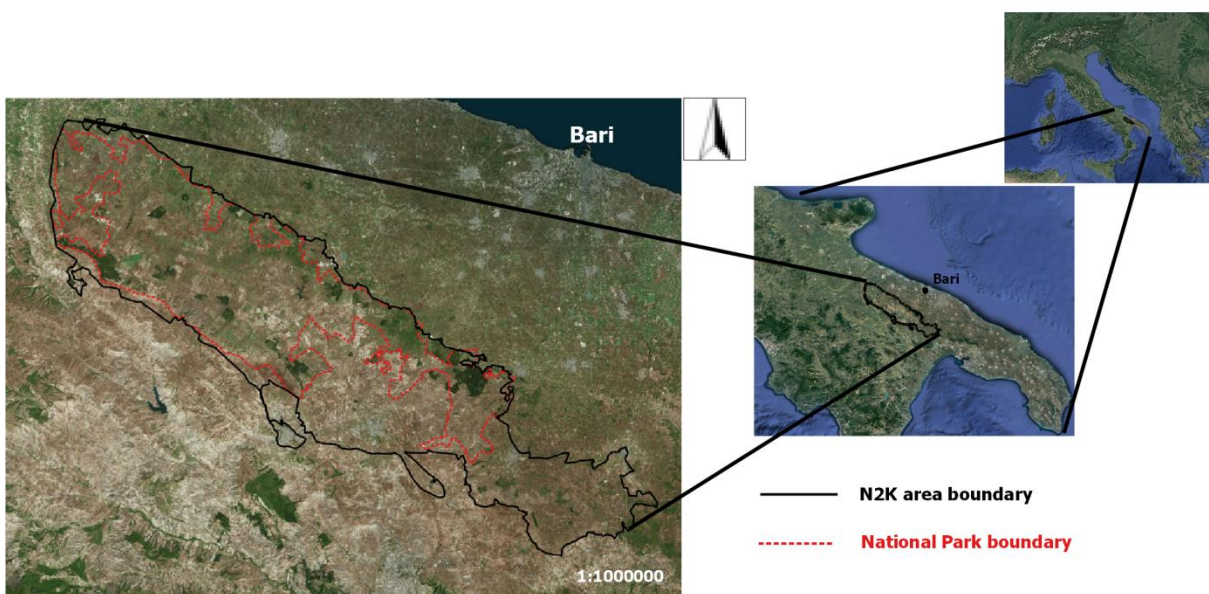
Figure 13. "Alta Murgia" study site, southern Italy.

The altitude of the area is from 285 to 680 m above the sea level and its climate is mesomediterranean oceanic subcontinental pluviseasonal with dry to sub-humid ombrotype (Forte et al, 2005). The site is characterized by a typical Mediterranean agro-pastoral landscape with millennial land use history mainly occupied by semi-natural rocky dry grasslands (Figure 14), traditionally used as extensive pastures, while forest vegetation consists only of residual patches of downy oak (*Quercus pubescens s.l.*) woodlands and Aleppo pine (*Pinus halepensis*) plantations (Mairota et al., 2013). This area is considered of crucial importance for the conservation of wildlife and priority species (Council Directive, 2009). In "Murgia Alta" the semi-natural grassland ecosystem hosts numerous regionally endemic and generally rare species,

but also many with trans-Adriatic distribution (Forte et al, 2005). During the last three decades, this unique ecosystem has been exposed to tremendous impacts and accelerated processes of habitat degradation, fragmentation and biotic contamination (i.e., woody encroachment), both within and next to its borders. As a result of the combined pressures, ecosystems are threatened or even in danger of destruction (Mairota et al., 2015).

Figure 14. "Alta Murgia" landscape.

The pressures related to degradation range from:

- the Common Agricultural Policy (CAP) which has driven the transformation of grassland pastures into agricultural (cereal crops intensification) areas by stone (rock) graining (clearance) that has induced soil erosion and sediment deposition in the aquifer system;
- the illegal waste and toxic mud dumping on transformed areas has caused heavy metal contamination of soils and aquifers;
- the increasing of traditional legal and illegal mining activities, wind farms infrastructures and arson;
- the below long-term average rainfall as a result of climate change;
- the spreading of invasive species (Tarantino et al., 2019; LifeWatch ERIC Validation Case, 2021).

Hence, the following indices and sub-indicators, reported in Table 7, has been selected spanning a period over the last 30 years for trend in LC and over the last 20 years for trend in phenology.

Table 7. Indices and sub-indicators selected for "Alta Murgia" study site.

Sub-indicators	Sensor	Spatial resolution (m)	Spatial frame	Temporal frame	Ground truth data	Annotations
LAND COVER MAP (focusing on Grasslands)	LANDSAT	30	N2K +5 km buffer	1990; 2001; 2004; 2011 (4 multi-seasons images per year)	Available ground data	• Temporal framework according to CLC products for comparison purposes. • 2004: Institution National Park
	LANDSAT; SENTINEL-2	30;10		2018 (4 multi-seasons images)		
	SENTINEL-2	10		2021 (4 multi-seasons images)		
GRASSLAND HABITAT MAP	SENTINEL-2	10	Subset where ground data are available	2018; 2021 (4 multi-seasons images and intra-annual time-series)		
BURNED AREAS COVER TREND	LANDSAT; SENTINEL-2	30;10	N2K +5 km buffer	2000-2021 (inter-annual time series)	Archive from state forestry service	
VEGETATION PHENOLOGY TREND			Only for those LC classes for which ground		ARIF database or new in field acquisitions (accumulation chamber)	

VEGETATION SUFFERING ESTIMATION (PRI;SIF)	MODIS; PRISMA	1000 (MODIS, daily acquisitions); 30 (PRISMA, monthly acquisitions)	data are available		New in field acquisitions (accumulation chamber)	• Possible super-resolution or pansharpened techniques for PRISMA data • spring and autumn measures (2021-2022)- correlation with primary production.
HISTORICAL CLIMATE ANALYSIS	Chelsa and ERA5 Land	1km (Chelsa); 9km (ERA5-Land)	N2K +5 km buffer	Daily stats 1981-2005; Hourly 1979-2021	Local weather station	
SOC	SENTINEL-2; PRISMA	10	Only for those LC classes for which ground data are available	2020	Available ground data (2020)	Possible super-resolution or pansharpened techniques for PRISMA data

For the monitoring of recovery actions by NBS, that will be implemented in Alta Murgia site, due to the small size of the areas involved, VHR images will be considered acquiring on demand commercial Pléiades or Worldview-2/3 satellite images.

Worldview-3 is the first commercial ultra-high-resolution satellite with 26 super-spectral bands and large acquisition capabilities. Launched in 2014, WorldView-3 is one of the orbiting satellites

by DigitalGlobe; it is capable of acquiring images at a panchromatic resolution of 31 centimetres, 1.24 meters multispectral (Vis/NIR), 3.7 meters shortwave infrared (SWIR) and 30 meters CAVIS (Clouds, Aerosols, Vapors, Ice, and Snow). With an average revisit time of less than 1 day, WorldView-3 is able to acquire up to 680,000 km² per day.

The two high-resolution satellites, Pléiades-1A and Pléiades-1B, were launched by Airbus Defence & Space on the 2011 latest. This constellation is capable of providing images acquired in panchromatic at 70 centimetres resolution and in multispectral (Vis+NIR) at 2.8 meters resolution, with a daily revisit time of any point on Earth. In addition, the Pléiades satellites are able to acquire high-resolution stereo images in a single pass.

5.2   Palo Laziale (Italy)

The N2K site "Bosco di Palo Laziale" (SCI IT6030022) is located along the coastline of the Lazio Region, in the Metropolitan area of Rome, about 40 km NW of Italy's capital, within the Municipality of Ladispoli (Figure 15). It is a flat area of about 130 hectares with an altitude between 3 and 10 meters above sea level and about 100 meters away from the coastline.

According to the bioclimatic features, the area is located within the Mediterranean region, as defined by the compensated summer ombrothermic index (Rivas Martìnez, 2008). During the summer, the high temperatures and the low precipitation give rise to a dry period and negative water balance of the soil due to the high evapotranspiration.

Lithology shows an alternation of alluvial and deltaic sediments with different permeability. Sands and biocalcarenites of the Middle Pliocene (Macco formation), alluvial deposits and sand layers of the Pleistocene, coastal sand and polygenic pebbles reworked with volcanic elements of the Holocene are all more permeable. In contrast, the quaternary deposits consisting of clay, silt and clay of lakes and marshes, peat and cemented sand may be considered of low permeability (Figure 16).
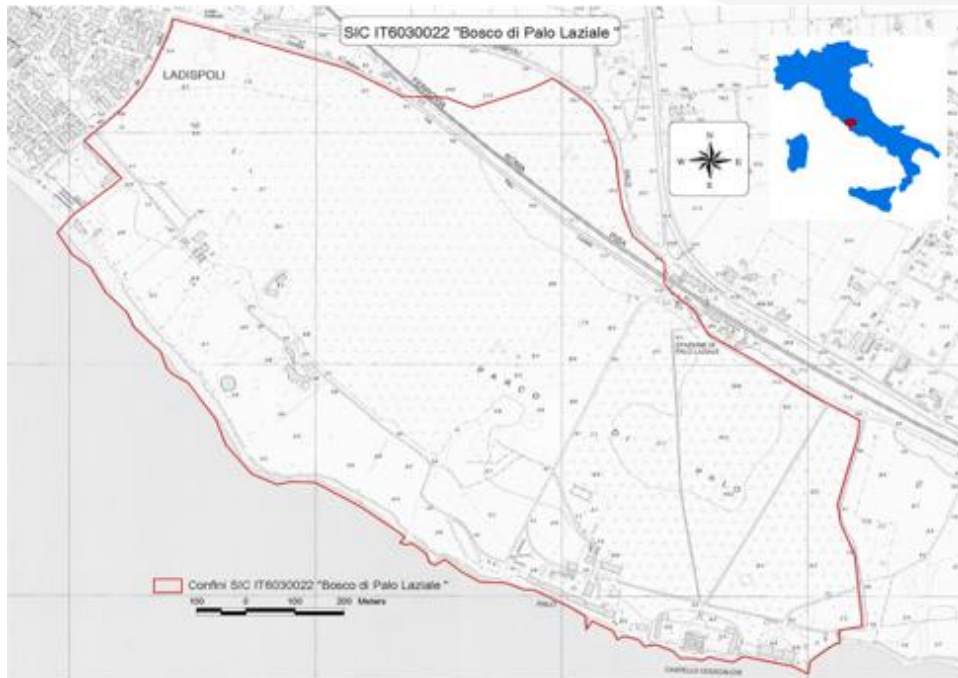
Figure 15. Boundary of N2K site "Bosco di Palo Laziale" (Ladispoli), Rome, Italy.

Figure 16. "Palo Laziale": a) Geologic section with the outcrop of Macco formation; b) Sclerophyll's vegetation margin with field of Phalaridetalia coerulescentis and Thero-Brachypodietea; c) An aerial view of Palo Laziale.

The site's core area is set within an entirely fenced-off private property representing one of the last remainings of an ancient Mediterranean floodplain forest that was progressively reduced over the centuries by reclamation and deforestation activities. Such a peculiar example of

coastal forest of western-central Italy is primarily composed of mixed oak formations, including *'Pannonian-Balkanic turkey oak-sessile oak forests*' (habitat type 91M0), *'Mediterranean holm-oak forests*' (9340) and *'Thermophilous Fraxinus angustifolia woods*' (91B0) (Figure 17). Moreover, the site presents small and ephemeral habitat types which are particularly rich in biodiversity, such as the *'Mediterranean temporary ponds*' (*3170) and the *'Natural euthrophic lakes with Magnopotamion or Hydrocharition-type vegetation'* (3150) (Figure 16). The forest offers shelter to a large variety of animal species of which many of them are listed in the Annex II of the Habitat Directive, such as the Hermann's tortoise (*Testudo hermanni*), the European pond turtle (*Emys orbicularis*), or Jersey tiger moth (*Euplagia quadripunctaria*), all protected under Annex I of the Habitats Directive, and many other species listed in the Birds Directive.

Figure 17. "Palo Laziale": a) Narrow-leaved ash forest communities; b) A view of the habitat 91M0.

Over the last decades, the area has been increasingly exposed to unexpected changes in the climate regimes that altered the sustainable fluctuation of precipitation and drought. As a result, due to constantly increasing temperatures and extreme fluctuations of the rainfalls, the site has been affected by a tremendous case of aridity, especially at the soil level which also turned into an increasing vulnerability to fires. This has triggered a serious case of forest

dieback in Palo Laziale with manifold adverse effects in the vegetation, habitats and associated wildlife, including bush encroachment and over-competition for trophic resources in the forest stands. In addition, several heat waves had caused high mortality in the trees of Palo Laziale in the last 20 years, such as the summer of 2003 when about 40% of the adult trees were found died – also due to the concomitant negative effect of fungal agents, such as *Discula quercina* and *Diploidia corticola*. The fungal infection was a secondary source of forest decline induced by the stressed metabolic condition of the trees due to the aridity.

From 2018, a set of restoration interventions have been carried out in the site in the framework of the EU-funded project LIFE PRIMED (LIFE17 NAT/GR/000511). At that time, the forest looked more like a savanna than a floodplain oak woodland, with about 80% of the original canopy being lost and the survived trees showing high senescence and low seed production. Most of the topsoil freed by the dominant tree layer was occupied by thorny shrubs (e.g., *Rubus spp.*), with only limited free areas available for new saplings to grow. There was forest regeneration (plants at least three years old), but the shrubs suffocated growing seedlings. Such an encroachment strongly inhibited forest recovery and threatened the area occupied by the temporary ponds. Such an invasion caused burial of the shallow ponds leading to water eutrophication, decreasing photosynthesis sunlight and limiting gas exchange between the water surface and the atmosphere.

The following indices and sub-indicators, reported in Table 8, has been selected. Due to the small size of the study site (< 50 ha) VHR satellite data will be used.

Table 8. Indices and sub-indicators selected for "Palo Laziale" study site.

Sub-indicators	Sensor	Spatial resolution (m)	Spatial frame	Temporal frame	Ground truth data	Annotations

LAND COVER MAP (focusing on Forests)	PLEIADES	2	N2K +1 km buffer	2020-2021 (4 multi-seasons images)	Available ground data	
HABITAT MAP						
VEGETATION PHENOLOGY TREND	QUICKBIRD	2.4		2002-2009 (1 image per year)		2004: sick trees cutting
BURNED AREAS COVER TREND	LANDSAT; SENTINEL-2	30;10		2002-2021 (inter annual time series)		
LAI ESTIMATIONS	SENTINEL-2 (by Sen2Cor)	10	Only for those LC classes for which ground data are available	2015; 2020	Canopy Evapo-transpiration ->LAI (2020)	
FAPAR ESTIMATIONS (for GPP)	SENTINEL-2; PRISMA				Available ground data (2020)	Possible super-resolution or pansharpened techniques for PRISMA data
HISTORICAL CLIMATE ANALYSIS	Chelsa and ERA5 Land	1km (Chelsa); 9km (ERA5-Land)	N2K +5 km buffer	Daily stats 1981-2005; Hourly 1979-2021	Local weather station	

SOC	SENTINEL-2; PRISMA	10	Only for those LC classes for which ground data are available	2019; 2021	Available ground data (2019)	Possible super-resolution or pansharpened techniques for PRISMA data

5.3   Nestos (Greece)

The Delta of the river Nestos is an alluvial area of high ecological significance of about 55,000 ha created over the centuries by the gradual accumulation of deposits from the mainland towards the sea. The Nestos river is considered one of the most important rivers in Greece. It originates from Mount Rila (2,716 m), southern Bulgaria and flows into the Thracian Sea, forming a natural boundary between Macedonia and Thrace, in northeastern Greece. It is 234 km in length and its basin covers an area of 574,900 ha, of which 130 km and 228,000 ha lies in the Greek territory (Samaras & Koutitas, 2008). Because of its size and the variety of its habitats, the Nestos Delta is considered among the most important wetlands of Greece and Europe. Its ecological significance is reflected by the two N2K sites it forms: the Habitats Directive site (SCI) "DELTA NESTOU KAI LIMNOTHALASSES KERAMOTIS - EVRYTERI PERIOCHI KAI PARAKTIA ZONI" (GR1150010) (23,043.86 ha) and the Birds Directive site (SPA) "DELTA NESTOU KAI LIMNOTHALASSES KERAMOTIS KAI NISOS THASOPOULA" (GR1150001) (14,783.79 ha) (Figure 18).

Figure 18. "Nestos" NATURA 2000 sites, GR1150001 and GR1150010, in the study area.

A significant feature of the SCI GR1150010 is the riparian forest known as "Kotza Orman" (Great Forest), one of the largest of its type in the Mediterranean area. Despite being reduced, through land reclamation and hydraulic changes in the river functions, from 12,000 ha in the early 1920s to merely 2,000 ha in fragments along both banks of the river, it is still the largest natural riparian forest in Greece. Part of project LIFE02 NAT/GR/008489 included reforestation in public lands along the river with indigenous species to increase the size of the forest. In total 60 ha of new forest were created. Parts of the reforested areas were fenced to prevent access and vegetation has grown abundantly.

According to the Monitoring Report for Terrestrial Habitats in the area of the SCI GR1150010 occurs 28 habitat types, including priority ones such as "Coastal lagoons" (1150*), "Mediterranean temporary ponds" (3170*), "Allluvial forests with *Alnus glutinosa* and *Fraxinus excelsior*" (*Alno-Padion, Alnion incanae, Salicion albae*) (91E0*) (Figure 19).

Figure 19. Within the "Nestos" Delta: a) The 91E0* & 3170* priority habitats in SCI GR1150010 NATURA 2000; b) Alluvial forest (91E0*); c) temporary pond (3170*)

The Nestos Delta is also very important from an ornithological perspective because of its great area and variety of habitat types. It is a significant part of the wetland chain in northern Greece, extending from the Aliakmonas-Axios complex to the Evros Delta. As many as 300 bird species have been recorded as nesting, overwintering, or migrating through this region, 34 of which are endangered and strictly protected raptors. Most of these species are protected by national, European, and international legislation. A large number is included in the Red Data Book of Threatened Vertebrates of Greece, and 103 species are listed under the Bern Convention, out of which 75 are included in Directive 2009/149/EC. The Nestos delta hosts the last pure wild

population of Black-necked Pheasant *Phasianus colchicus colchicus* in Europe, a remnant closely related to wild populations in its natural range in central Asia. *Phasianus c. colchicus* is listed in the Red Data Book of Threatened Vertebrates of Greece as critically endangered, and the population is estimated at 100-250 individuals.

Three mammals have been included as very important species (listed in Annex II of the 92/43/ECC Habitats Directive): the Eurasian otter (*Lutra lutra*) and 2 marine mammals, harbour porpoise (*Phocoena phocoena*) and common bottlenose dolphin (*Tursiops truncatus*). The conservation status for the Eurasian otter, the only of these species connected to the temporary pond, is average or reduced.The reptile and amphibian fauna are very rich, with 11 species of amphibians and 22 species of reptiles. Species of Annex II of the Directive 92/43/EEC include *Testudo graeca*, *Elaphe quatuorlineata*, *Elaphe situla*, *Mauremys rivulata*, *Zamenis situla*, *Bombina bombina* and *Triturus karelinii*. *Emys orbicularis*, which is in part dependent on the temporary pond habitat, is classified as near threatened both at the Mediterranean level (IUCN) and in the Red Data Book of Threatened Vertebrates of Greece. *Eurotestudo hermanni* is classified as near threatened in the Mediterranean region (IUCN) and vulnerable in Greece in the Red Data Book. There are 21 freshwater fish species in the river Nestos of which have been included as very important species (listed in Annex II of the 92/43/ECC Habitats Directive): *Barbus strumicae*, European bitterling (*Rhodeus amarus*), Bulgarian spined loach (*Cobitis strumicae*), twaite shad (*Alosa fallax*) and Mediterranean killifish (*Aphanius fasciatus*). The conservation status for these species in the area is good (B), except for twaite shad whose conservation status is average or reduced. Fourteen species are autochthonous, and 6 are endemic. Another 36 euryhaline and marine fish species have been identified in the lagoons and the river estuary. Two invertebrates have been included as very important species (listed in Annex II of the 92/43/ECC Habitats Directive): the green snaketail dragonfly (*Ophiogomphus cecilia*) and bladetail dragonfly (*Lindenia tetraphylla*). The conservation status for these species in the area is good.

According to the mapping analysis of Mallinis et al. (2011) for the broad area of the Nestos Delta, during the first period of their analysis (1945-1960), agricultural areas increased, rangelands (often used as pastures) expanded, while forests and wetlands decreased. Furthermore, an increase in alluvial areas, especially in the river mouth, was noticed. These

changes correspond to major socio-economic changes occurring in northern Greece at that time (800,000 refugees who settled into the wider area of Macedonia following the Asia Minor catastrophe in 1922). During that time, around 1933, the river course was re-aligned to its present position, while, swamps were drained and irrigation infrastructures were developed, thus changing the river's flow regime. Additionally, between 1945 and 1960, the Kotza Orman riparian forest was cut down in order to cover increased needs for agricultural land. During the second period of the (Mallinis et al., 2011) study (1960-1992), an irrigation and regulatory dam (Toxotes) was constructed in the Delta's neck (1960-1966). During this period, the extent of areas being cultivated was increased and rangelands decreased. Simultaneously, a change of the spatial location of agricultural fields (swap change) to the most fertile and accessible areas is evident, along with an increase in their mean patch size. Additionally, alluvial areas decreased in cover after the dam construction due to changes in the discharge regime and reduction of the sediment load. Finally, in the third period of the study (1992-2002), a gross loss of agricultural areas was observed and alluvial areas were further reduced due to two large dams on the Nestos River (170 m and 95 m in height) which reduced the river's sediment load (Xeidakis & Delimani, 2002).

The habitat types of Nestos are thus very sensitive to modifications of the hydrological cycle due to both direct and indirect pressures (e.g. inappropriate river management, climate change, respectively) since their life cycle depends on the regular alternation of wet and dry phases. For instance, during winter 2016-2017, the ponds held water for only about 2 months, compared to the average (about 6 months), and their typical vegetation did not have the opportunity to complete its life cycle. On the other hand, in alluvial forest habitat (91E0*), the lack of flooding also means no transport of nutrient-rich sediments, which enrich the soils.

Furthermore, the uncontrolled expansion of shrubs affects both the 3170* and the 91E0* habitat types. Another problem is the illegal logging and trampling that affects the forest structure and the temporary ponds, respectively, which has noticeably increased in recent years because of the economic crisis and lack of local people's awareness about their importance. In the end, there is also the problem of the Invasive Alien Species. The number of

these species amounts to three (*A. fruticosa, P. dioica, A. negundo*), and they are outcompeting indigenous species, mainly in 91E0*, but also encroaching on 3170* (Figure 20).

Figure 20. Amorpha fruticosa extended by a temporary pond (3170) in "Nestos" Delta.*

From 2018, these pressures and threats are targeted by a set of restoration interventions that are under implementation in the framework of the EU-funded project LIFE PRIMED (LIFE17 NAT/GR/000511). These measures include the development of hydraulic system to make the ecosystem more resilient to the external pressures, installation of information boards and awareness-raising campaign to reduce illegal logging and trampling, field assessment and control by removal of invasive plant species.

The following indices and sub-indicators, reported in Table 9, has been selected.

Table 9. Indices and sub-indicators selected for "Nestos" study site.

Sub-indicators	Sensor	Spatial resolution (m)	Spatial frame	Temporal frame	Ground truth data	Annotations

LAND COVER MAP	LANDSAT; SENTINEL-2	30;10		2000;2005;2010;2017;2021	Available ground data	
INVASIVE SPECIES MAP			N2K +5 km buffer	2018; 2021-2022	Drone acquisitions	In 2020 (Autumn) cutting of invasive species starts
HYDRO-PERIOD INDEX	SENTINEL-2	10		October 2017-september 2018; October 2019-september 2020; October 2021-september 2022	Available ground data	
SOIL SALINITY INDICES	SENTINEL-2	10	Only for bare soil or herbaceous areas	2018; 2020; 2022	No	
LAI ESTIMATIONS	SENTINEL-2 (by Sen2Cor)	10	Only for those LC classes for which ground data are available	2015; 2021	Canopy Evapo-transpiration ->LAI (2021)	

HISTORICAL CLIMATE ANALYSIS	Chelsa and ERA5 Land	1km (Chelsa); 9km (ERA5-Land)	N2K +5 km buffer	Daily stats 1981-2005; Hourly 1979-2021	Local weather station	

5.4 Asterousia (Greece)

The Asteroussia Mt range is located in the Heraklion Prefecture of Crete spanning a zone 55 km long in the East-West and 5-10 km wide in the North-South direction, along the southern coastline of Crete. Four subset areas will be analysed in the project (red boundaries in Figure 21). The 72% of the area is a N2K site (SPA: GR4310013 SAC: GR4310004 and GR4310005) and 3 Wildlife Refuges are delineated, the Asterousia and Kofinas K706, Vigla-Kryo Nero Antiskari - K587 and West Asterousia-Agiofaraggo.

Project area: Asteroussia Mt.
Surface area (ha): 52,000
SPA: GR4310013
SAC: GR4310004
         GR4310005
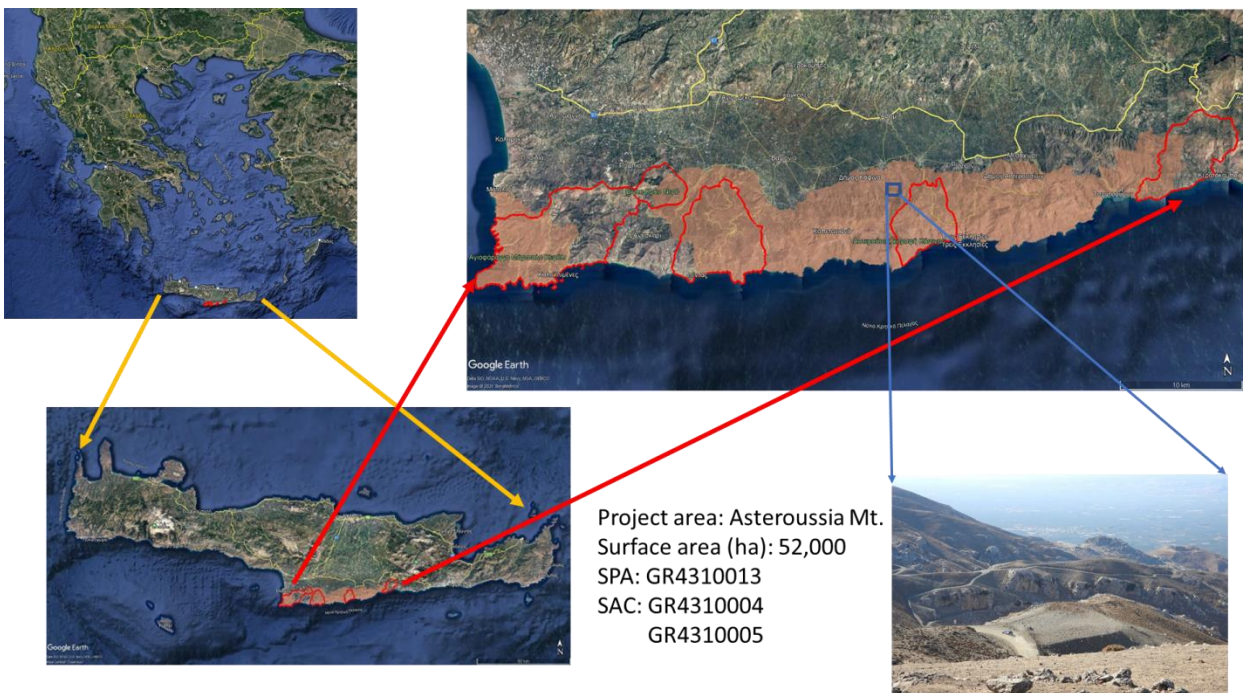
Figure 21. "Asterousia" site. The four subset areas analysed are overlaid in red boundaries.

Until 1920, the slopes of Asteroussia were cultivated with cereals and legumes. Due to low productivity, grains cultivation has been abandoned along with the associated traditional terraced fields and the area is currently used mainly as grazing land for sheep and goat herds.

The climate of the area is characterized as sub-humid Mediterranean with humid and relatively cold winters and dry and warm summers.

The most important land cover types are natural grasslands, sclerophylous vegetation, transitional woodland-shrubland, and sparsely vegetated areas. Natural vegetation consists mainly of shrubs and some isolated maquis and pine forests. In areas with relatively deep soils, old vineyards and continuously expanding greenhouses and olive groves are present. Although the natural vegetation in the Asteroussia Mt range shows a capacity for succession to higher forms, this is not the case since the area is overgrazed especially during the winter months when more animals are transferred from surrounding areas.

Asteroussia Mt range soils are generally shallow, with the dominant depth class being 15-30 cm (70% of the area) with few patches of deeper soils (class 30-60 cm) and have high amounts of rock fragments: 57% of the area falls in the 40-60% rock fragment content class and 43% in the 15-40% class. Soil is predominantly fine textured (84%) and to a lesser degree medium textured (16%).

Topographically, the area is characterized by steep slopes, very steep cliffs and steep torrents. The highest peak, Kofinas, rises to 1231 m. About 22% of the area has elevation up to 200 m, about 36% has elevation of 200-400 m and elevations above 800 m cover only about 5% of the area. The Asteroussia Mt range is covered by composite landforms with level land accounting for 44% of the area, slopes 26% and steep land 30% (Figure 22).

The Asteroussia Mt range climatic conditions, with long, dry summers and high evapo-transpiration rates, favor desertification. The loss of productive, arable land from soil erosion and degradation and the over exploitation of aquifers are among the key factors posing a desertification risk for the site which is, subsequently, further intensified by climate deregulation and raising global temperatures.

Figure 22. "Asterousia" landscape.

The key pressures and main land degradation processes affecting the study area are: a) decline in vegetation cover/biomass and over grazing resulting from the increase of livestock numbers; b) landscape modification, soil erosion and soil organic matter decline due to anthropogenic interventions such as installation of new olive groves and greenhouses, opening of new roads, expansion of coastal tourism settlements, installation of Renewable Energy Sources facilities; c) accidental or intentional (for scrubland clearance) wildfires; d) hydrological modification; e) soil salinization due to overexploitation of aquifers.

The following indices and sub-indicators, reported in Table 10, has been selected.

Table 10. Indices and sub-indicators selected for "Asterousia" study site.

Sub-indicators	Sensor	Spatial resolution (m)	Spatial frame	Temporal frame	Ground truth data	Annotations
LAND COVER MAP	LANDSAT; SENTINEL-2	30;10	4 subsets areas	2000;2005;2010;2017;2021	Available ground data	
BURNED AREAS COVER TREND				2000-2021 (inter-annual time series)	No	
VEGETATION PHENOLOGY TREND	MODIS; LANDSAT; SENTINEL-2	1000;30;10		Before and after fire events	No	Possible correlation between phenology trend and agricultural primary products (meat, honey, milk etc. available for 2010 and presumably for 2022)
SOIL SALINITY INDICES	SENTINEL-2	10	Only for bare soil or herbaceous areas	2018;2020;2022	No	

5.5 El Bruc (Spain)

The regions of Anoia and El Bages suffered a serious fire in July 2015, which burned 1,235 between the municipalities of El Bruc, Òdena, Castellfollit del Boix, Sant Salvador de Guardiola and Castellolí, on the perimetral area of the Montserrat Natural Park (included in the Montserrat-Roques Blanques-riu Llobregat Natura 2000 site, with code ES5110012). A large part of the burned forest was a pine forest of Aleppo pine (*Pinus halepensis*), which had already

suffered a fire in 1986. The pines - which do not have a regrowth strategy, but rather germinate - are having a modest and variable regeneration throughout the region. Within the framework of the LIFE The Green Link project (LIFE15 CCA/SE/125), more than 20 ha of forest and agricultural species were planted to recover the most degraded areas and favour the recovery of the agro-silvo-pastoral mosaic, which helps reduce the vulnerability of the area facing upcoming forest fires.

The area affected by the fire is located in the central area of Catalonia (Spain) (Figure 23), characterized by a dry sub-humid climate, with an average rainfall of between 600 and 700 mm per year, and located at an altitude of between 450 and 500 meters above sea level.
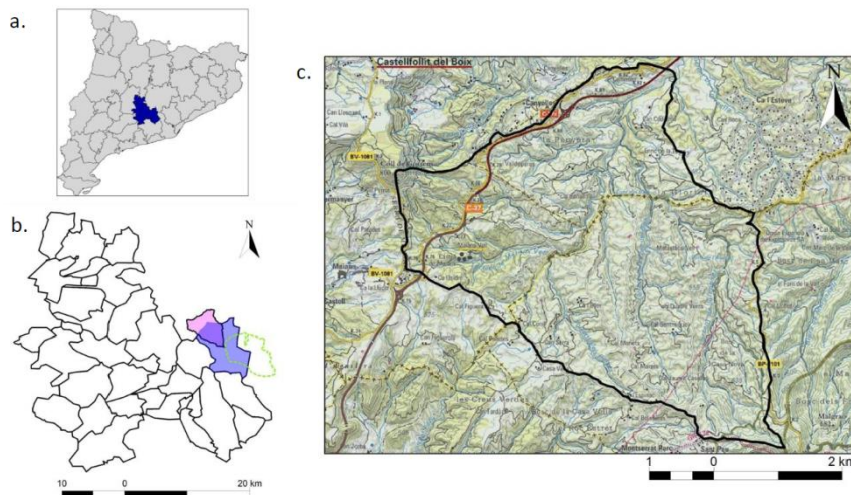
Figure 23. a) General location of Anoia region in Catalonia, Spain; b) Location of "El Bruc" municipality (blue poligon) in the context of Anoia region, Monserrat Natural Park limits (green) and area affected by 2015 forest fire (rose); c) Limits of the area affected by 2015 forest fire represented in 1:50.000 topographic map (ICGC, 2021).

There is an average of less than 50 days of rain per year, with frequent periods of drought and water stress by the plants, which have been increased in recent years. Due to this factor, as well as the high recurrence of forest fires, it presents areas with low natural regeneration and affected by processes of concentrated and diffuse erosion. In addition, like many areas of the Mediterranean, and especially of the Iberian Peninsula, this area is affected by rural abandonment since the beginning of the 19th century, which has caused an expansion of the forest, mainly of Aleppo pine, which increases the risk of large forest fires. Hence the interest

in promoting environmental restoration projects that favour the restoration of cultivated fields, as well as the forest management of the wooded masses. The clearings in Aleppo pine reforestation not only help the regeneration after fires or other disturbances, but also promote the good structure and dynamics of the forest (Figure 24).
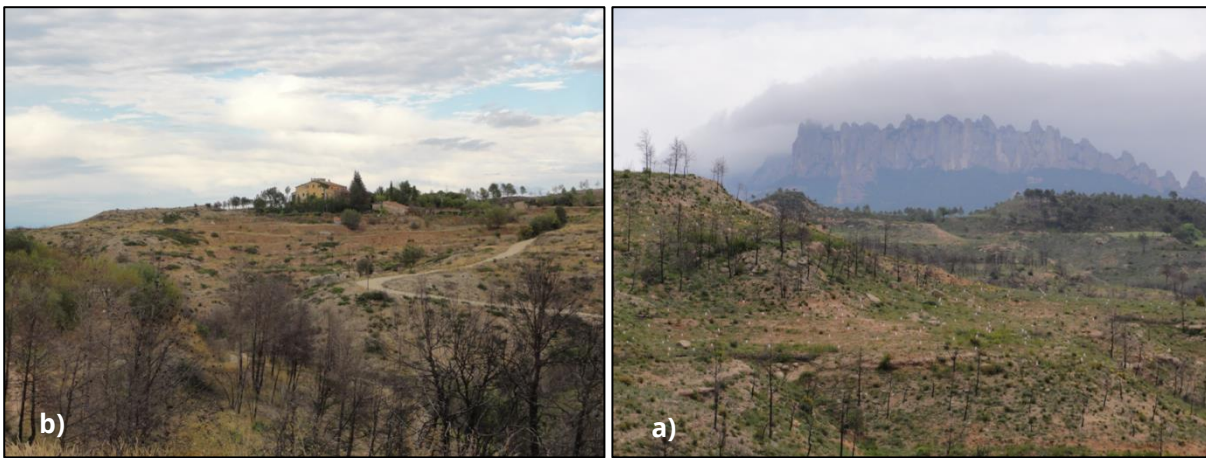
Figure 24. a) General view of one of the areas planted in the context of LIFE The Green Link (May2017); b) Detail of one of the areas severely affected by erosion processes after the forest fire (July 2016).

The following indices and sub-indicators, reported in Table 11, has been selected.

Table 11. Indices and sub-indicators selected for "El Bruc" study site.

Sub-indicators	Sensor	Spatial resolution (m)	Spatial frame	Temporal frame	Ground truth data	Annotations

LAND COVER MAP	LANDSAT; SENTINEL-2	30;10	N2K +5 km buffer	2014;2016;2021	Available ground data	Important fire event in 2015
BURNED AREAS COVER TREND				2014-2021		
SEEDLINGS PHYSIOLOGICAL STATE				2016-2021	Ground data from 2017, 2018, 2019	
VEGETATION PHENOLOGY TREND	MODIS; LANDSAT; SENTINEL-2	1000;30;10		Before and after fire events	Vegetation cover measures in 2017, 2018 and 2019	
SOC	SENTINEL-2	10	Only for those LC classes for which ground data are available	2017;2019;2021	If sufficient validation data are available (2017; 2019)	

5.6   Tifaracas (Gran Canaria, Spain)

Tifaracás is a desertified area located in the municipality of Artenara, on the island of Gran Canaria (Figure 25). It is located within the El Nublo Rural Park, which in turn is included in the Gran Canaria Biosphere Reserve. The area is classified as a Site of Community Interest (SCI) and a Special Conservation Area (ZEC), included in the N2K Network (site code ES7010039).

Figure 25. Location map of "Tifaracás" in Gran Canaria island (red point).

Although the area has a high risk of desertification, we find vegetation typical of the arid and semi-arid environments of the island, with a predominance of herbaceous species, although with a very low cover. In the framework of the LIFE The Green Link project (LIFE15 CCA/SE /125) more than 4,000 seedlings of native forest species, trees and shrubs, were planted using the "Cocoon" system (Figure 26 and 27). The objective of the plantation is to reverse desertification processes and improve the ecological connectivity of the adjacent Canary Island pine forests. The area is severely affected by desertification processes, which are aggravated by reduced rainfall, recurrent forest fires and herbivore caused by the abundant presence of wild goats. Average annual rainfall is below 200 mm, although in recent years it has not exceeded 100 mm. In recent years, dry periods, without rainfall, have lasted more than 10 months, which difficult the reforestation efforts that try to establish a vegetation cover in order to protect the soil from the erosion. Although soils are not particularly vulnerable to erosion due to the high stoniness, the low vegetation cover, the steep slopes of the slopes and the torrential rains favour erosive processes. These processes cause the loss of fertile soil, which makes it even more difficult to establish a vegetation cover.

Figure 26. Steep slopes and stony soils where Cocoons were installed in Tifaracás (May 2017).

Figure 27. Details of: (a) seedlings of Pinus canariensis and (b) Juniperus turbinata subsp. canariensis planted with the Cocoon device. See the fences installed around the seedlings to protect them against wild goats (July 2018).The following indices and sub-indicators, reported in Table 12, has been selected.

Table 12. Indices and sub-indicators selected for Tifaracas study site.

Sub-indicators	Sensor	Spatial resolution (m)	Spatial frame	Temporal frame	Ground truth data	Annotations
LAND COVER MAP	LANDSAT; SENTINEL-2	30;10	N2K +5 km buffer	2005; 2011; 2014; 2017; 2021	Available ground data	
BURNED AREAS COVER TREND				2005-2021		
SEEDLINGS PHYSIOLOGICAL STATE				2016-2021	Ground data from 2017, 2018, 2019	
VEGETATION PHENOLOGY TREND	MODIS; LANDSAT; SENTINEL-2	1000;30;10		Before and after fire events	Vegetation measures in 2017 and 2019	
SOC	SENTINEL-2	10	Only for those LC classes for which ground data are available	2017;2019;2021	If sufficient validation data are available (2017; 2019)	

6.   Protocol of guidelines for remote sensing indicators identification in the LD assessment at local scale

Resuming the analysis emerged in the searching for indicators from remote sensing to assess LD, at local scale, a protocol with a series of guidelines can be outlined as below:

1. Definition of the spatial frame identifying the boundary of the Area Of Interest (AOI) and a buffer area around:
   a. Case of AOI > 50 hectares size: a 5 km wide buffer area around;
   b. Case of AOI < 50 hectares size: a 1 km wide buffer area around.
2. Definition of the temporal frame to be monitored identifying eventual trigger events and setting the baseline to determine the initial status.
3. Selection of the optical satellite images (and their radiometric and geometric calibration) to be considered:
   a. Case of AOI > 50 hectares size:
      i. Case of long term monitoring, back in time before 2015: Landsat satellite data must be considered
      ii. Case of monitoring from 2015: Sentinel-2 satellite data can be considered
   b. Case of AOI < 50 hectares size: VHR commercial satellite data need to be considered.
4. Definition of the scale of detail: local site-scale.
5. Identification of pressures and threats for the specific site by expert-knowledge.
6. List of LC classes according to the taxonomy selected.
7. Collecting all the available ground truth data useful for validation.
8. Review for indices/indicators/methods from remote sensed data in recent literature.
9. Identification of sub-indicators for the SDG 15.3.1 evaluation, according to the main pressures and to the available validation data for each site.
10. Identification of methodologies (pixel/object – based; data-driven/knowledge-driven approach) and computation techniques (e.g., machine learning) to adopt for extracting the sub-indicators for each site.
11. List of the main changes of interest (from-to transitions) to be monitored.

12. Integration of all sub-indicators converging into the SDG 15.3.1 indicator by summing all areas subjected to "negative" change (i.e., degraded) and dividing by the total land area using "One Out, All Out" area-based principle for each sub-indicator.

7.   Gaps and strengths in the protocol

Different sources of gaps can arise in the protocol application:

- Availability of optical satellite data without cloud cover or considering clouds/clouds shadow masking;
- Need of tasking and purchase for VHR satellite data in case of small size of study areas;
- Difficulties in the radiometric and geometric calibration mainly for VHR data and in case of mountainous sites (topographic correction);
- Difficulty in the validation of sub-indicators for the lack of ground truth data mainly in the past: in particular for SOC or NPP or their proxies in-field measures;
- Difficulty in the training of data-driven machine learning algorithms due to the lack of sufficient ground truth data;
- Difficulty in obtaining finer land cover details without ancillary data or sufficient information to discriminate among the classes;
- Possibility to obtain soil salinity indices (soil measures sub-indicator) only for those areas covered by bare soil or herbaceous vegetation (the presence of dense trees does not allow to observe the soil from satellite);
- Lack of validation data for SOC, soil salinity, burned areas and vegetation phenology trend indices for the Greek sites due to slight control of the territory;
- Need to update the list of sub-indicators as the sites change.

Essentially, the strength of the protocol lies in its strong local scale characterisation:

- Starting from an accurate analysis of the main problems affecting the different types of Mediterranean ecosystems;
- Provisioning for local scale detail: HR or VHR satellite data in case of areas > 50 ha or < 50 ha, respectively;
- Increase of sub-indicators to be combined to obtain SDG 15.3.1;
- Calculation of SDG 15.3.1 indicator at local scale overcoming the current Trends.Earth tool available at global scale;
- Usefulness for local decision-makers.

8.   Conclusion

Remote sensing plays a key role in the NewLife4Drylands project for the LD assessment. Its essential contribution is that monitoring is no longer carried out exclusively by photo-interpretation and expensive and difficult field analysis.

In the first nine months of the projects some main challenges have been addressed by A2 action:

1) working at a local scale, in order to meet the needs of local decision-makers offering a more reliable evaluation of the LD status than is currently possible by using freely available products (e.g., Copernicus services produced on a pan-European scale);

2) do not searching for new methodologies for LD assessment but rather decline on a local scale those well known in literature;

3) assessing what can be done using freely available open satellite data as much as possible.

Therefore, supported by the experts who know the study areas, the problems of each individual site have been analysed and pressures and threats identified. A sort of protocol of guidelines for the identification, at local scale, of specific sub-indicators extracting from remote sensing data for each site, by selecting open satellite data everywhere possible, has been outlined. The sub-indicators will be integrated for the evaluation of the SDG 15.3.1 indicator as recommended by UNCCD.

The protocol do not represent a site-specific solution but, rather, it is conceived for application to whatever site providing guidelines for the approach at local scale. The six study sites of the project, hosting a wide variety of ecosystem types (drylands, coastal, mountainous, with high or low extension, affected by specific treats causing LD), offer the opportunity for investigations appropriate for Mediterranean landscape.

9.   Aknowledgements

References

Adamo, M.; Tarantino, C.; Tomaselli, V.; Veronico, G.; Nagendra, H.; Blonda, P. (2016). Habitat mapping of coastal wetlands using expert knowledge and Earth observation data. J. Appl. Ecol., 53, 1521–1532.

Adamo, M.; Tarantino, C.; Tomaselli et al. (2014). Expert knowledge for translating land cover/use maps to general habitat categories (GHC). Landsc. Ecol., 29, 1045–1067.

Assennato, F.; Di Leginio, M.; D'Antona, M.; Marinosci, I.; Congedo, L.; Riitano, N.; Luise, A.; Munafò, M. (2020). Land degradation assessment for sustainable soil management. Italian Journal of Agronomy 2020, Vol. 15:1770

Aquilino, M.; Adamo, M.; Blonda, P.; Barbanente, A.; Tarantino, C. (2021). Improvement of a Dasymetric Method for Implementing Sustainable Development Goal 11 Indicators at an Intra-Urban Scale. Remote Sensing, Special Issue "Earth Observations for Sustainable Development Goals", 13, 2835, https://doi.org/10.3390/rs13142835

Bai, Z.G. & Dent, D.L. (2009). Recent land degradation and improvement in China. AMBIO - A Journal of the Human Environment, 38(3), 150–157. doi:10.1579/0044-7447-38.3.150

Bai, Z.G.; Dent, D.L.; Olsson, L. & Schaepman, M.E. (2008). Proxy global assessment of land degradation. Soil Use and Management, 24(3), 223–234. doi:10.1111/sum.2008.24.issue-3

Bannari, A.; Morin, D.; Bonn, F.; Huete, A.R. (1995). A review of vegetation indices. Remote Sens. Rev. 13, 95–120. https://doi.org/10.1080/02757259509532298

Bhunia, G.S.; Shit, P. K.; Pourghasemi, H. R. (2017). Soil organic carbon mapping using remote sensing techniques and multivariate regression model. Geocarto International 34(2). DOI: 10.1080/10106049.2017.1381179

Bishop, C.M. (1996). Neural Networks for Pattern Recognition. Oxford University Press

Brown, M.E.; de Beurs, K.; Vrieling, A. (2010). The response of African land surface phenology to large scale climate oscillations. Remote Sensing of Environment, 114 (10), 2286–2296. doi:10.1016/j.rse.2010.05.005

Chen, D.; Huang, J.; Jackson, T. J. (2005). Vegetation water content estimation for corn and soybeans using spectral indices derived from MODIS near- and short-wave infrared bands. Remote Sens. Environ., 98, 225– 236.

Chen, W.; Liu, L.; Zhang, C.; Pan, Y. (2004). Monitoring the seasonal bare soil areas in Beijing using multitemporal TM images. Proceedings Geoscience and Remote Sensing Symposium, IGARSS 2004.

Copernicus ESA Program. Available online: https://www.esa.int/Applications/Observing_the_Earth/Copernicus (accessed on 22 June 2018)

Council Directive 2009/147/EEC:

Available online: https://eur-lex.europa.eu/legalcontent/EN/TXT/?uri=CELEX%3A32009L0147

Deng, Y.; Wu, C.; Li, M.; Chen, R. (2015). RNDSI: A ratio normalized difference soil index for remote sensing of urban/suburban environments. International Journal of Applied Earth Observation and Geoinformation, vol. 39, pp. 40–48, 2015

Di Gregorio, A.; Jansen, L.J.M. (2005). Land Cover Classification System (LCCS): Classification Concepts and User Manual. Food and Agriculture Organization of the United Nations: Rome, Italy.

Douaoui, A.; Lepinard, P. (2010). Remote sensing & soil salinity: mapping of soil salinity in the Algerian plain "Lower-Cheliff". Geomatics Expert, 76: 36–41.

Douaoui, A.E.K.; Nicolas, H.; Walter, C. (2006). Detecting salinity hazards within a semiarid context by means of combining soil and remote-sensing data. Geoderma 134:217–230

Dubovyk, O. (2017). The role of Remote Sensing in land degradation assessments: opportunities and challenges. European Journal of Remote Sensing, Vol.50, No. 1, 601-613

Dubovyk, O., Menz, G., Conrad, C., Kan, E., Machwitz, M., & Khamzina, A. (2013a). Spatio-temporal analyses of cropland degradation in the irrigated lowlands of Uzbekistan using remote-sensing and logistic regression modeling. Environmental Monitoring and Assessment, 185(6), 4775–4790. doi:10.1007/s10661-012-2904-6

Elhag, M. (2016). Evaluation of Different Soil Salinity Mapping Using Remote Sensing Techniques in Arid Ecosystems, Saudi Arabia. Journal of Sensors, 96175–96175, 2016.

Fazzini, P.; De Felice Proia, G.; Adamo, M.; Blonda, P.; Petracchini, F.; Forte, L.; Tarantino, C. (2021). Sentinel-2 Remote Sensed Image Classification with Patchwise Trained ConvNets for Grassland Habitat Discrimination. Remote Sensing, Special Issue "Deep Learning for Remote Sensing Image Classification", 13(12), 2276. https://doi.org/10.3390/rs13122276

Forte, L.; Perrino, E.V.; Terzi, M. (2005). Le praterie a Stipa austroitalica Martinovsky ssp. austroitalica dell'Alta Murgia (Puglia) e della Murgia Materana (Basilicata). Fitosociologia, 42, 83–103

Gamon, J.; Penuelas, J.; Field, C.B. (1992). A Narrow-Waveband Spectral Index That Tracks Diurnal Changes in Photosynthetic Efficiency. Remote Sensing of Environment 41(1):35-44. DOI: 10.1016/0034-4257(92)90059-S

Gao, J. & Liu, Y. (2010). Determination of land degradation causes in Tongyu County, Northeast China via land cover change detection. International Journal of Applied Earth Observations and Geoinformation, 12(1), 9–16. doi:10.1016/j.jag.2009.08.003

Gao, B. (1996). NDWI—A normalized difference water index for remote sensing of vegetation liquid water from space. Remote Sensing of Environment, Vol. 58, Issue 3, December 1996, Pages 257-266. https://doi.org/10.1016/S0034-4257(96)00067-3

Gavish, Y.; O'Connel, J.; Marsh, C.J.; Tarantino, C.; Blonda, P.; Tomaselli, V.; Kunin, W.E. (2018). Comparing the performance of flat and hierarchical Habitat/Land-Cover classification models in a NATURA 2000 site. ISPRS Journal of Photogrammetry and Remote Sensing, 136, 1-12. https://doi.org/10.1016/j.isprsjprs.2017.12.002

Gholizadeh, H.; Gamon, J.; Zygielbaum, A.; Wang, R. (2018). Remote sensing of biodiversity: Soil correction and data dimension reduction methods improve assessment of α-diversity (species richness) in prairie ecosystems. Remote Sensing of Environment, 206, 240-253, DOI:10.1016/j.rse.2017.12.014

Gillanders, S.N.; Coops, N.C.; Wulder, M.A.; Gergel, S.E. & Nelson, T. (2008). Multitemporal remote sensing of landscape dynamics and pattern change: Describing natural and anthropogenic trends. [Review]. Progress in Physical Geography, 32(5), 503–528. doi:10.1177/0309133308098363

Gitelson, A.; Kaufman, Y.J.; Merzlyak, M.N. (1996). Use of a green channel in remote sensing of global vegetation from EOS-MODIS. Remote Sensing of Environment, Vol. 58, Issue 3, p. 289-298. https://doi.org/10.1016/S0034-4257(96)00072-7

Giuliani, G.; Egger, E.; Italiano, J.; Poussin, C.; Richard, J.P.; Chatenoux, B. (2020a). Essential Variables for Environmental Monitoring: What Are the Possible Contributions of Earth Observation Data Cubes? Data, 5, 100. doi:10.3390/data5040100

Giuliani, G.; Mazzetti, P.; Santoro, M.; Nativi, S.; Van Bemmelen, J.; Colangeli, G.; Lehmann, A. (2020b). Knowledge generation using satellite earth observations to support sustainable development goals (SDG): A use case on Land degradation. Int. J. Appl. Earth OBS. Geoinformation, 88. https://doi.org/10.1016/j.jag.2020.102068

Gu, Y.; Brown, J. F.; Verdin, J. P.; Wardlow, B. (2007). A five-year analysis of MODIS NDVI and NDWI for grassland drought assessment over the central Great Plains of the United States, Geophys. Res. Lett., 34, L06407

Higginbottom, T.P. & Symeonakis, E. (2014). Assessing land degradation and desertification using vegetation index data: Current frameworks and future directions. [Review]. Remote Sensing, 6(10), 9552–9575. doi:10.3390/rs6109552

ICGC (2021). Mapa topogràfic de Catalunya 1:50.000. Available in: https://www.icgc.cat/Administracio-i-empresa/Descarregues/Cartografia-topografica/Mapa-topografic-1-50.000

ISPRA (2014). Manuali e Linee Guida 109/2014, pp.43. ISBN 978-88-448-0649-1

Jiang, Z.; Huete, A.; Didan, K.; Miura, T. (2008). Development of a two-band enhanced vegetation index without a blue band. Remote Sensing of Environment, 112(10):3833-3845. DOI: 10.1016/j.rse.2008.06.006

Karavitis, C.A.; Tsemelis, D.E. et al. (2014). Linking drought characteristics to impacts on a spatial and temporal scale. Water Policy 16, 1172–1197. doi: 10.2166/wp.2014.205

Karnieli, A.; Bayarjargal, Y.; Bayasgalan, M.; Mandakh, B.; Dugarjav, C.; Burgheimer, J.; Gunin, P.D. (2013). Do vegetation indices provide a reliable indication of vegetation degradation? A case study in the Mongolian pastures. International Journal of Remote Sensing, 34(17), 6243–6262. doi:10.1080/01431161.2013.793865

Key, C.H.; Benson, N.; Ohlen, D.; Howard, S.; Mckinley, R.; Zhu, Z. (2002). The normalized burn ratio and relationships to burn severity: ecology, remote sensing and implementation. Proceedings of the Ninth Forest Service Remote Sensing Applications Conference. American Society for Photogrammetry and Remote Sensing, Bethesda, MD

Khan, N.M.; Rastoskuev, V.V.; Shalina, E.V.; Sato, Y. (2001). Mapping salt-affected soils using remote sensing indicators - a simple approach with the use of GIS IDRISI. Ratio. 5–9

Lastovicka, J.; Svec, P.; Paluba, D.; Kobliuk, N.; Svoboda, J.; Hladaky, R.; Stych, P. (2020). Sentinel-2 Data in an Evaluation of the Impact of the Disturbances on Forest Vegetation. Remote Sensing, 12, 1914. doi:10.3390/rs12121914

Le, Q.B.; Nkonya, E. & Mirzabaev, A. (2016). Biomass productivity-based mapping of global land degradation hotspots. In E. Nkonya, A. Mirzabaev, & J. von Braun (Eds.), Economics of land degradation and improvement – A global assessment for sustainable development (pp. 55–84). Cham: Springer International Publishing.

Li, D.; Shan, J. & Li, J.G. (Eds.). (2009). Geospatial technology for earth observation. New York, NY: Springer.

LifeWatch ERIC Validation Case. (2021). https://www.lifewatch.eu/web/guest/escience-for-nis-research-workshop-speakers

Luo, T.; Pan, Y.; Ouyang, H. et al. (2004). Leaf area index and net primary productivity along subtropical to alpine gradients in the Tibetan Plateau. Global Ecology and Biogeography, 13 , 345–358

Main, R.; Cho, M.A.; Mathieu, R.; O'Kennedy, M.M.; Ramoelo, A.; Koch, S. An investigation into robust spectral indices for leaf chlorophyll estimation. ISPRS J. Photogramm. Remote Sens. 2011, 66, 751–761. https://doi.org/10.1016/j.isprsjprs.2011.08.001

Mairota, P.; Cafarelli, B.; Labadessa, R.; Lovergine, F.; Tarantino, C.; Lucas, R.; Nagendra, H.; Didham, R. (2015). Very high resolution Earth observation features for monitoring plant and animal community structure across multiple spatial scales in protected areas. Int. J. Appl. Earth Obs. Geoinf., 37, 100–105

Mairota, P.; Leronni, V.; Xi, W.; Mladenoff, D.; Nagendra, H. (2013). Using spatial simulations of habitat modification for adaptive management of protected areas: Mediterranean grassland modification by woody plant encroachment. Environ. Conserv., 41, 144–146.

Mallinis, G.; Emmanoloudis, D.; Giannakopoulos, V.; Maris, F.; Koutsias, N. (2011). Mapping and interpreting historical land cover/land use changes in a Natura 2000 site using earth observational data: The case of the Nestos delta, Greece. Applied Geography 31: 312 – 320

McDowell, N.G.; Coops, N.C.; Beck, P.S.A.; Chambers, J. Q.; Gangodagamage, C.; Hicke, J.A.; Meddens A.J. (2015). Global satellite monitoring of climate-induced vegetation disturbances. [Review]. Trends in Plant Science, 20(2), 114–123. doi:10.1016/j.tplants.2014.10.008

McFeeters, S.K. (1996). The use of the Normalized Difference Water Index (NDWI) in the delineation of open water features. International Journal of Remote Sensing, vol. 17, no. 7, pp. 1425–1432. https://doi.org/10.1080/01431169608948714

MEA Millennium Ecosystem Assessment. (2005). Global Assessment Report: Policy Responses. In: Millennium Ecosystem Assessment, Island Press, Washington, D.C. pp. 213-255 https://digitalarchive.worldfishcenter.org/handle/20.500.12348/1918?show=full

NASA USGS Portal. Available online: https://earthexplorer.usgs.gov/ (accessed on 9 May 2018).

Niphadkar, M.; Nagendra, H.; Tarantino, C.; Adamo, M.; Blonda, P. (2017). Comparing pixel and object-based approaches to map an understorey invasive shrub in tropical mixed forests. Frontiers in Plant Science, Research Topic Remote Sensing of invasive species, 8: 892. doi:10.3389/fpls.2017.00892

Nkonya, E.; Mirzabaev, A. & von Braun, J. (2016a). Economics of land degradation and improvement: An introduction and overview. In E. Nkonya, A. Mirzabaev, & J. von Braun (Eds.), Economics of land degradation and improvement – A global assessment for sustainable development (pp. 1–14). Cham: Springer International Publishing.

Prince, S.D.; Wessels, K.J.; Tucker, C.J. & Nicholson, S.E. (2007). Desertification in the Sahel: A reinterpretation of a reinterpretation. Global Change Biology, 13(7), 1308– 1313. doi:10.1111/gcb.2007.13.issue-7

Qi, J.; Chehbouni, A.; Huete, A.R.; Kerr, Y.H.; Sorooshian, S. (1994). A modified soil adjusted vegetation index. Remote Sensing of Environment, vol. 48, no. 2, pp. 119–126. https://doi.org/10.1016/0034-4257(94)90134-1

Reed, M.S.; Buenemann, M.; Atlhopheng, J.; Akhtar-Schuster, M.; Bachmann, F.; Bastin, G.; Evely, A.C (2011). Cross-scale monitoring and assessment of land degradation and sustainable land management: A methodological framework for knowledge management. Land Degradation & Development, 22(2), 261–271. doi:10.1002/ldr.1087

Renza, D.; Martinez, E.; Arquero, A.; Sanchez, J. (2010). Drought Estimation Maps by Means of Multidate Landsat Fused Images. Remote Sensing for Science, Education, and Natural and Cultural Heritage, EARSEL, pp. 775-782

Reynolds, J.; Smith, D.; Lambin, E.; Turner, B.; Mortimore, M.; Batterbury, S. ; Huber-Sannwald, E. (2007). Global desertification: Building a science for dryland development. Science, 316(5826), 847–851. doi:10.1126/science.1131634

Reynolds, J.F.; Grainger, A.; Stafford Smith, D.M., et al. (2011). Scientific concepts for an integrated analysis of desertification. Land Degradation and Development, 22(2), 166–183. doi:10.1002/ldr.1104

Rivas-Martínez, S. (2008). Global Bioclimatics (Clasificación Bioclimática de la Tierra). http://www.globalbioclimatics.org/book/bioc/global_bioclimatics-2008_00.htm.

Rondeaux, G.; Steven, M.; Baret, F. (1996). Optimization of soil-adjusted vegetation indices. Remote Sensing of Environment, vol. 55, no. 2, pp. 95–107. https://doi.org/10.1016/0034-4257(95)00186-7

Rouse, J. W.; Haas, R. H.; Schell, J. A.; Deering, D. W. (1974). Monitoring vegetation systems in the Great Plains with ERTS. NASA special publication, vol. 351(1), pp. 309-317

Safriel, U. (2007). The assessment of global trends in land degradation. In M.K. Sivakumar & N. Ndiang'ui (Eds.), Climate and land degradation (pp. 1–38). Berlin Heidelberg: Springer

Samaras, A. G. & Koutitas, C. G. (2008). Modelling the impact on coastal morphology of the water management in transboundary river basins: the case of River Nestos. Management of Environmental Quality, 19(4), 455 – 466

SDG 15.3.1. (2021). Version 2.0 – Good Practice Guidance. SDG Indicator 15.3.1, Proportion of Land That Is Degraded Over Total Land Area. Available online on 29 September 2021 from:

https://www.unccd.int/publications/good-practice-guidance-sdg-indicator-1531-proportion-land-degraded-over-total-land

Symeonakis, E. (2021). Special Issue Information of Remote Sensing journal "Land Degradation Assessment with Earth Observation", ISSN 2072-4292, https://www.mdpi.com/journal/remotesensing/special_issues/land_degradation_assessment_earth_observation

Sivakumar, M. & Stefanski, R. (2007). Climate and land degradation. Berlin: Springer.

Stavi, I. & Lal, R. (2015). Achieving zero net land degradation: Challenges and opportunities. Journal of Arid Environments, 112(PA), 44–51. doi:10.1016/j.jaridenv.2014.01.016

Tarantino, C.; Forte, L.; Blonda, P.; Vicario, S.; Tomaselli, V.; Beierkuhnlein, C.; Adamo, M. (2021). Intra-Annual Sentinel-2 Time-Series Supporting Grassland Habitat Discrimination", Remote

Sensing, Special Issue "Remote Sensing for Habitat Mapping, 13(2), 277, ISSN: 2072-4292, https://doi.org/10.3390/rs13020277

Tarantino, C.; Casella, F.; Adamo, M.; Lucas, R.; Beierkuhnlein, C.; Blonda, P. (2019). Ailanthus altissima mapping from multi-temporal very high resolution satellite images. ISPRS Journal of Photogrammetry and Remote Sensing. https://doi.org/10.1016/j.isprsjprs.2018.11.013

Tarantino, C.; Adamo, M.; Lucas, R.; Blonda, P. (2016 a). Detection of changes in semi-natural grasslands by cross correlation analysis with Worldview-2 images and new Landsat 8 data. Remote Sensing of Environment, Vol. 175C, pp. 65-72. doi: 10.1016/j.rse.2015.12.031

Tarantino, C.; Lovergine, F.; Niphadkar, M.; Lucas, R.; Nativi, S.; Blonda, P. (2016 b). Towards Operational Detection of Forest Ecosystem Changes in Protected Areas. Remote Sensing, 8(10), 850, doi:10.3390/rs8100850

Thaler, E.A.; Larsen, I.J.; Yu, Q. (2019). A New Index for Remote Sensing of Soil Organic Carbon Based Solely on Visible Wavelengths. Soil Sci. Soc. Am. J. 83:1443–1450. doi:10.2136/sssaj2018.09.0318

Tsesmelis ,D.E.; Karavitis, C.A.; Oikonomou, P.D.; Alexandris, S.; Kosmas, C. (2018). Assessment of the Vulnerability to Drought and Desertification Characteristics Using the Standardized Drought Vulnerability Index (SDVI) and the Environmentally Sensitive Areas Index (ESAI). Resources, 8, 6. doi:10.3390/resources8010006

Tian, F.; Cai, Z.; Jin, H. et al. (2021). Calibrating vegetation phenology from Sentinel-2 using eddy covariance, PhenoCam, and PEP725 networks across Europe. Remote Sensing of Environment, 260, 112456. DOI: 10.1016/j.rse.2021.112456

Tomaselli, V.; Dimopoulos, P.; Marangi, C.; Kallimanis, A.S.; Adamo, M.; Tarantino et al. (2013). Translating land cover/land use classifications to habitat taxonomies for landscape monitoring: A Mediterranean assessment. Landsc. Ecol. 2013, 28, 905–930

Trends.Earth. (2018). Conservation International. Available online at: http://trends.earth

Tüshaus, J.; Dubovyk, O.; Khamzina, A. & Menz, G. (2014). Comparison of medium spatial resolution ENVISAT-MERIS and terra-MODIS time series for vegetation decline analysis: A case study in central asia. Remote Sensing, 6(6), 5238–5256. doi:10.3390/rs6065238

UNCCD. (1994). Elaboration of an international convention to combat desertification in countries experiencing serious drought and/or desertification, particularly in Africa. Bonn: UN

UNCCD. (2015). Report of the Conference of the Parties on its twelfth session, held in Ankara from 12 to 23 October 2015. Part two: Actions taken by the Conference of the Parties at its twelfth session. ICCD/ COP(12)/20/Add. Bonn: United Nations Convention to Combat Desertification. Available from: https://www2.unccd.int/sites/default/files/sessions/documents/ICCD_COP12_20_Add.1/20add 1eng.pdf

UNCCD. (2017). Good Practice Guidance. SDG Indicator 15.3.1: Proportion of Land That Is Degraded Over Total Land Area. Version 1.0 September 2017. Available from: http://www2.unccd.int/sites/default/files/relevant-links/2017-10/Good%20Practice%20Guidance_SDG%20Indicator%2015.3.1_Version%201.0.pdf

UNCCD. (2018). The LDN Target Setting Programme. Website of the United Nations Convention to Combat Desertification (UNCCD). Available from: https://www.unccd.int/actions/ldn-target-setting-programme

UNCCD. (2021). Good Practice Guidance for National Reporting on UNCCD Strategic Objective 3. To mitigate, adapt to, and manage the effects of drought in order to enhance resilience of vulnerable populations and ecosystems. Available online on 29 September 2021 from: https://www.unccd.int/publications/good-practice-guidance-national-reporting-unccd-strategic-objective-3-mitigate-adapt

Vapnik, V.N. (1998). Statistical Learning Theory; Wiley: New York, NY, USA

Vapnik, V.N. (1995). The Nature of Statistical Learning Theory; Springer: New York, NY, USA

Vibhute, A.D., Dhumal, R., Nagne, A., Surase, R., Varpe, A., Gaikwad, S. (2017). Evaluation of Soil Conditions using Spectral Indices from Hyperspectral Datasets. 2nd International Conference on Man and Machine Interfacing (MAMI)

Vicario, S.; Adamo, M.; Alcaraz-Segura, D.; Tarantino, C. (2020). Bayesian Harmonic Modelling of Sparse and Irregular Satellite Remote Sensing Time Series of Vegetation Indexes: A Story of Clouds and Fires. Remote Sensing, Special Issue "Remote Sensing in Ecosystem Modelling", 12(1), 83. doi:10.3390/rs12010083

Viscarra Rossel, R.; Behrens, T. (2010). Using data mining to model and interpret soil diffuse reflectance spectra. Geoderma, 158, 46-54

Vlek, P.; Le, Q. & Tamene, L. (2008). Land decline in Land-Rich Africa: A creeping disaster in the making.
Rome: CGIAR Science Council Secretariat

Vogt, J.V.; Safriel, U.; Von Maltitz, G.; Sokona, Y.; Zougmore, R.; Bastin, G.; Hill, J. (2011). Monitoring and assessment of land degradation and desertification: Towards new conceptual and integrated approaches. Land Degradation & Development, 22(2), 150–165. doi:10.1002/ldr.1075

Vohland, M.; Ludwig, M.; Thiele-Bruhn, S.; Ludwig, B. (2017). Quantification of soil properties with hyperspectral data: Selecting spectral variables with different methods to improve accuracies and analyze prediction mechanisms. Remote Sensing, 9, 1103

Vohland, M.; Besold, J.; Hill, J.; Fründ, H.-C. (2011). Comparing different multivariate Calibration methods for the determination of soil organic carbon pools with visible to near infrared spectroscopy. Geoderma, 166, 198-205

Wessels, K.J.; van den Bergh, F. & Scholes, R.J. (2012). Limits to detectability of land degradation by trend analysis of vegetation index data. Remote Sensing of Environment, 125 (1), 10–22. doi:10.1016/j.rse.2012.06.022

Wu, J.; Liu, Y.; Wang, J., He, T. (2010). Application of Hyperion data to land degradation mapping in the Hengshan region of China. International Journal of Remote Sensing, vol. 31(19), pp. 5145-5161

Wunder, S.; Bodle, R. (2019). Achieving land degradation neutrality in Germany: Implementation process and design of a land use change based indicator. Env. Sci. Policy 92:46-55

Xeidakis, G. S. & Delimani, P. (2002). Coastal erosion problems in Northern Aegean coastline, Greece. The case of the Rhodope Prefecture coasts. Environmental Studies, 8: 151 - 158

Xu, H. (2006). Modification of normalised difference water index (NDWI) to enhance open water features in remotely sensed imagery. International Journal of Remote Sensing, Vol. 27, No. 14, 3025–3033

Yahiaoui, I.; Douaoui, A.; Zhang, Q.; Ziane, A. (2015). Soil salinity prediction in the Lower Cheliff plain (Algeria) based on remote sensing and topographic feature analysis. Journal of Arid Land, 7, pp. 794-805

Zhang, K. et al. (2019). Predicting Rice Grain Yield Based on Dynamic Changes in Vegetation Indexes during Early to Mid-Growth Stages. Remote Sensing, 11(4), 387. https://doi.org/10.3390/rs11040387

Zarco-Tejada, P.J.; Miller, J. R. et al. (2001). Estimation of chlorophyll fluorescence under natural illumination from hyperspectral data. Int. J. Appl. Earth Obs. Geoinf. 3, 321–327. https://doi.org/10.1016/S0303-2434(01)85039-X